LETTER

doi:10.1038/nature14021

Dauer-independent insulin/IGF-1-signalling implicates collagen remodelling in longevity

Collin Y. Ewald[1,2,3], Jess N. Landis[4]*, Jess Porter Abate[1,2,3]*, Coleen T. Murphy[4] & T. Keith Blackwell[1,2,3]

Interventions that delay ageing mobilize mechanisms that protect and repair cellular components[1–3], but it is unknown how these interventions might slow the functional decline of extracellular matrices[4,5], which are also damaged during ageing[6,7]. Reduced insulin/IGF-1 signalling (rIIS) extends lifespan across the evolutionary spectrum, and in juvenile *Caenorhabditis elegans* also allows the transcription factor DAF-16/FOXO to induce development into dauer, a diapause that withstands harsh conditions[1,2]. It has been suggested that rIIS delays *C. elegans* ageing through activation of dauer-related processes during adulthood[2,8,9], but some rIIS conditions confer robust lifespan extension unaccompanied by any dauer-like traits[1,10,11]. Here we show that rIIS can promote *C. elegans* longevity through a program that is genetically distinct from the dauer pathway, and requires the Nrf (NF-E2-related factor) orthologue SKN-1 acting in parallel to DAF-16. SKN-1 is inhibited by IIS and has been broadly implicated in longevity[12–14], but is rendered dispensable for rIIS lifespan extension by even mild activity of dauer-related processes. When IIS is decreased under conditions that do not induce dauer traits, SKN-1 most prominently increases expression of collagens and other extracellular matrix genes. Diverse genetic, nutritional, and pharmacological pro-longevity interventions delay an age-related decline in collagen expression. These collagens mediate adulthood extracellular matrix remodelling, and are needed for ageing to be delayed by interventions that do not involve dauer traits. By genetically delineating a dauer-independent rIIS ageing pathway, our results show that IIS controls a broad set of protective mechanisms during *C. elegans* adulthood, and may facilitate elucidation of processes of general importance for longevity. The importance of collagen production in diverse anti-ageing interventions implies that extracellular matrix remodelling is a generally essential signature of longevity assurance, and that agents promoting extracellular matrix youthfulness may have systemic benefit.

We hypothesized that SKN-1 would be required for rIIS lifespan extension under conditions in which dauer-associated processes are inactive. Class 2 mutations in the insulin/IGF-1 receptor DAF-2 induce adulthood dauer-related traits that are mild at 20 °C, and severe at 22.5 °C or above, but class 1 mutations do not (Supplementary Videos 1 and 2 and Supplementary Discussion)[10]. SKN-1 is inhibited by IIS phosphorylation but is dispensable for dauer development[13], adulthood dauer-related traits (Extended Data Fig. 1a–d and Supplementary Table 1), or lifespan extension by Class 2 *daf-2* mutations at 20 °C (Extended Data Fig. 1a and Supplementary Table 2)[13]. By contrast, at 15 °C SKN-1 was completely required for longevity in the same class 2 *daf-2* mutants (Fig. 1a, Extended Data Fig. 1a, e, Extended Data Table 1 and Supplementary Table 2), which do not show dauer traits at 15 °C (ref. 10) because low temperature inhibits dauer entry (Supplementary Discussion). The *skn-1* gene was also essential at 20 °C in class 2 *daf-16; daf-2* double mutants that expressed DAF-16 specifically in the intestine, a condition that rescues longevity but not dauer development[1,15] or traits (Extended Data Fig. 1f, g and Extended Data Table 1). Finally, *skn-1* was required at 15, 20, or 25 °C for lifespan extension from *daf-2* RNA interference (RNAi) (Fig. 1b, Extended Data Fig. 1a, Extended Data Table 1 and Supplementary Table 2), which promotes dauer entry only at extreme temperature and does not induce dauer traits in adults (Extended Data Fig. 1h–j). In these last two scenarios, the absence of dauer traits may reflect DAF-16 insufficiency in neurons, which are central to dauer regulation[15,16] and resistant to RNAi (Extended Data Fig. 1h, i and Extended Data Table 1). Lifespan extension is extremely robust when *daf-2* RNAi is performed in the class 1 mutant *daf-2*(*e1368*)[11], which lacks adulthood dauer traits but predisposes to dauer entry[10]. The *skn-1* gene was largely required for this lifespan extension at 20 °C, and was essential for the even greater healthy lifespan extension seen at 15 °C (117 days maximum; Fig. 1c, d, Extended Data Fig. 1a and Extended Data Table 1).

The *skn-1* dependence of rIIS longevity tracked inversely with predisposition to dauer entry or adulthood dauer traits, and was not determined

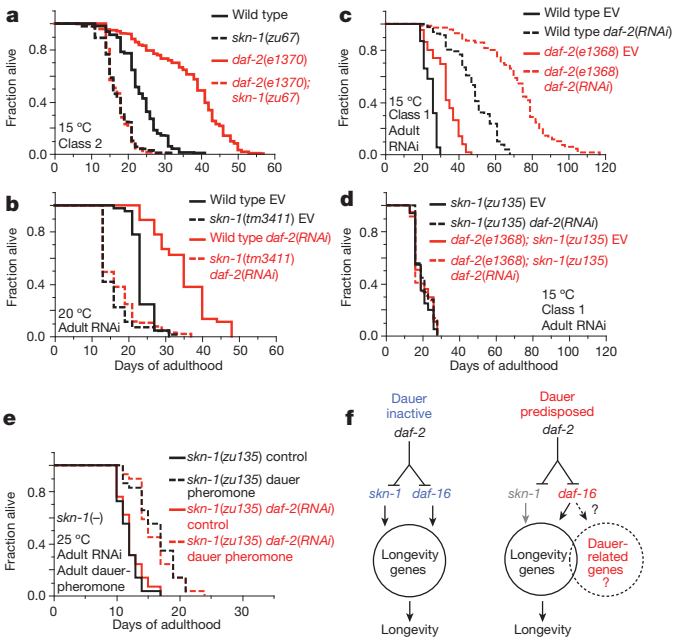

Figure 1 | Dauer-independent rIIS longevity requires SKN-1. a, **b**, The *skn-1* dependence of rIIS lifespan extension in the absence of dauer traits. **c**, **d**, The *skn-1* dependence of extreme rIIS longevity. EV, empty RNAi vector. **e**, The *skn-1* independence of longevity from adulthood dauer pheromone treatment but not *daf-2*(*RNAi*). **f**, Longevity assurance programs regulated by IIS. Under conditions that predispose to dauer traits (right), some SKN-1 functions may be assumed by DAF-16, possibly including ECM remodelling. Statistics and additional lifespan data are in Extended Data Table 1 and Supplementary Table 2.

[1]Joslin Diabetes Center, One Joslin Place, Boston, Massachusetts 02215, USA. [2]Harvard Stem Cell Institute, 7 Divinity Avenue, Cambridge, Massachusetts 02138, USA. [3]Department of Genetics, Harvard Medical School, 77 Avenue Louis Pasteur, Boston, Massachusetts 02215, USA. [4]Department of Molecular Biology, Lewis-Sigler Institute for Integrative Genomics, Princeton University, 148 Carl Icahn Laboratory, Washington Road, Princeton, New Jersey 08544, USA.
*These authors contributed equally to this work.

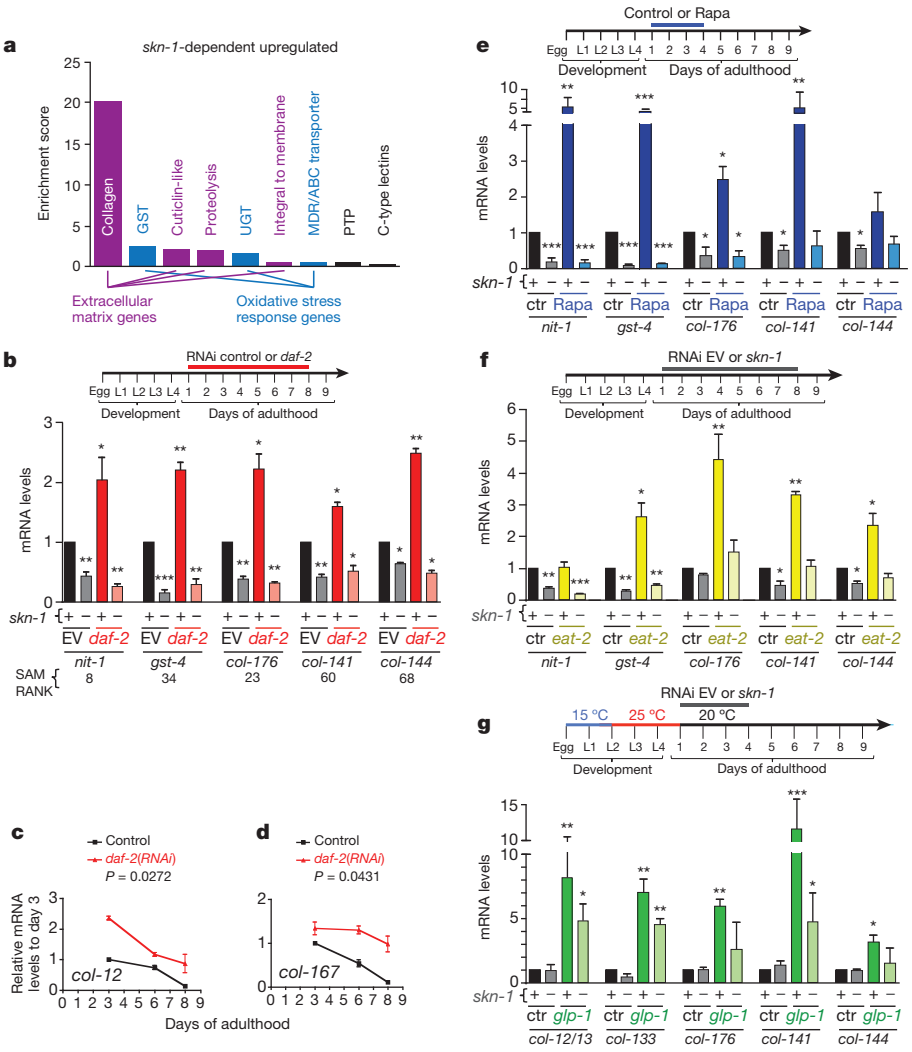

Figure 2 | Longevity-promoting interventions increase *skn-1*-dependent collagen expression in adults. **a**, Functional categories enriched in SKN-1-upregulated *daf-2*(−) gene sets, identified by the Database for Annotation, Visualization, and Integrated Discovery (DAVID). Enrichment scores of at least 1.3 are shown. **b**–**d**, Collagen upregulation by adulthood *daf-2* RNAi. Messenger RNA (mRNA) expression in wild-type (+) or *skn-1*(*zu135*) (−) animals, assayed by quantitative PCR (qPCR). The *nit-1* and *gst-4* genes are canonical SKN-1 targets[14,18]. Significance analysis of microarray (SAM) score ranks are in Supplementary Table 3. **e**, Rapamycin-treated (100 μM) wild-type and *skn-1*(*zu67*) animals are compared. **f**, Expression in the dietary restriction model *eat-2*. RNAi-sensitized control (*rrf-3*(*pk1426*)) (ctr) or *eat-2*(*ad1116*); *rrf-3*(*pk1426*) (*eat-2*) adults were exposed to empty RNAi vector or *skn-1* RNAi. **g**, Upregulation after germline stem-cell proliferation block induced by *glp-1*(*bn18*) temperature shift. Three replicates of 200 worms were analysed at the indicated days (**c**, **d**) or at the end of treatment. Data are mean ± s.e.m. $*P < 0.05$, $**P < 0.001$, $***P < 0.0001$ relative to wild type or control, by one-sample *t*-test, two-tailed, hypothetical mean of 1.

by temperature (Extended Data Fig. 1a). Also, *skn-1* dependence did not correlate with the magnitude of rIIS lifespan extension, suggesting that it was not determined by the extent of IIS reduction (Extended Data Fig. 1a). Accordingly, DAF-16 and SKN-1 nuclear localization was increased as robustly by *daf-2* RNAi as by class 1 or class 2 *daf-2* mutations, and was similar in *daf-2* mutants at 15 and 20 °C (Extended Data Fig. 1k–o). Activation of dauer processes in adults by a mechanism other than genetic IIS reduction should extend lifespan without *skn-1*. Accordingly, *skn-1* was dispensable for lifespan extension from adulthood dauer pheromone exposure (Fig. 1e, Extended Data Fig. 1p, q and Extended Data Table 1).

We conclude that *skn-1* is needed for rIIS longevity specifically when dauer-associated mechanisms are inactive (Extended Data Fig. 1a). This genetic requirement for *skn-1* reveals that rIIS extends lifespan through two downstream pathways that may overlap (Fig. 1f). During the reproductive life cycle, IIS inhibits a protective program that requires both DAF-16 and SKN-1, and does not involve dauer-specific processes. This

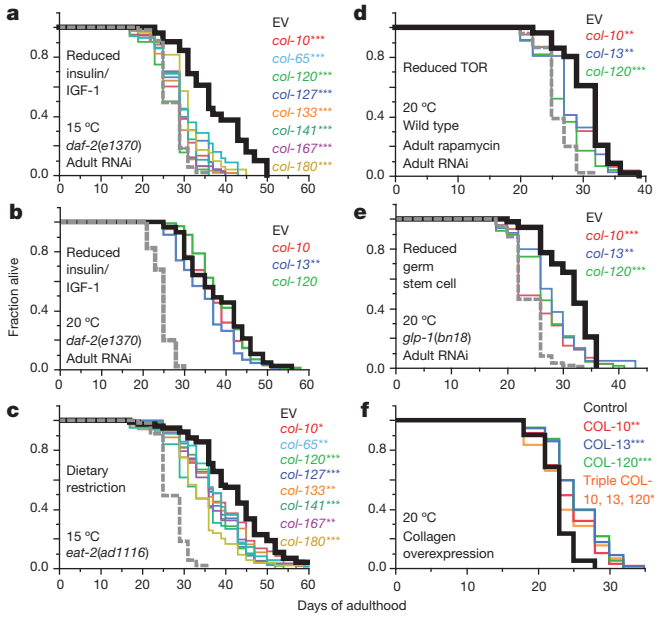

Figure 3 | Adulthood collagen expression promotes longevity. **a**, **b**, SKN-1-upregulated collagens are needed for *daf-2*(*e1370*) longevity at 15 but not 20 °C. **c**, Adulthood collagen knockdown reduced *eat-2*(*ad1116*) lifespan at 15 °C. Trial run in parallel with **a** and Extended Data Fig. 4c. **d**, Adulthood collagen expression is required for rapamycin lifespan extension. Rapamycin treatment and RNAi were initiated at adulthood day 1. **e**, Longevity from reduced germline stem cell number requires adult collagen expression. *glp-1*(*bn18*) was exposed to RNAi or empty RNAi vector control after downshift from the non-permissive temperature to 20 °C. In **a**–**e**, the grey dashed line shows the wild-type or control lifespan. **f**, Overexpression of collagens COL-10, COL-13, and COL-120 individually or in combination increased lifespan. $*P < 0.05$, $**P < 0.001$, $***P < 0.0001$ by log-rank. Statistics and additional lifespan data are in Extended Data Table 3 and Supplementary Table 13.

program may be controlled mainly by IIS acting outside the nervous system. The requirement for SKN-1 for lifespan extension is relieved under conditions that activate vestiges of the dauer developmental pathway in adults.

Analyses of how rIIS affects ageing have typically involved conditions that predispose to mild or even severe dauer-related traits (Supplementary Discussion), and would therefore allow *skn-1*-independent lifespan extension. We investigated the basis for dauer-independent rIIS longevity by identifying genes that are regulated by SKN-1 in *daf-2* mutants at 15 °C. At a false discovery rate of less than 3%, microarrays identified 429 genes with higher expression in *daf-2*(−) than *daf-2*(−); *skn-1*(−) animals (SKN-1-upregulated *daf-2*(−) genes), and 477 SKN-1-downregulated *daf-2*(−) genes, including direct and indirect SKN-1 targets (Extended Data Fig. 2a–e and Supplementary Table 3). Many of these genes affected lifespan as would be predicted by these expression patterns (Extended Data Fig. 2f–h and Supplementary Tables 4 and 5). Overlap with a dauer-expressed gene set was insignificant, as was overlap between SKN-1- and DAF-16-downregulated *daf-2*(−) genes (Extended Data Fig. 2i–k). However, many SKN-1-upregulated *daf-2*(−) genes were activated by DAF-16 (Extended Data Fig. 2j, l–t), which is also required for *daf-2* lifespan extension at 15 °C (ref. 17), indicating that SKN-1 responds to rIIS by functioning both in parallel to and independently of DAF-16.

SKN-1 has conserved functions in stress defence, protein homeostasis, and metabolism[12,18,19] and was required for *daf-2* oxidative stress resistance (Supplementary Table 6)[13], but only 40 out of 429 SKN-1-upregulated *daf-2*(−) genes had been identified under normal or stress conditions (Extended Data Fig. 3a–g and Supplementary Table 7)[18]. Unexpectedly, by far the most overrepresented functional group within the SKN-1-upregulated *daf-2*(−) gene set consisted of collagen genes, which seemed to be regulated by SKN-1 indirectly (Fig. 2a and Supplementary Tables 3, 8 and 9). In humans, collagens constitute about one-third of all protein and accumulate damage during ageing, leading to functional decline in tissues throughout the body[6,7]. *C. elegans* collagens form basement membranes as well as the cuticle, a complex structure that covers the animal, lines the buccal cavity, pharynx, and rectum, and becomes thickened and wrinkled with age[20]. The SKN-1-upregulated *daf-2*(−) collagens are of the type that forms the cuticle, but are expressed in multiple tissues (Extended Data Fig. 3h and Supplementary Table 9). Collagen production decreases in human skin during ageing[21], and 27 SKN-1-upregulated *daf-2*(−) collagens are among a set of genes that decline in expression as *C. elegans* ages[22] (Supplementary Table 10). These and other collagens were prominently upregulated in each of 20 *C. elegans* longevity-associated gene sets we examined (Extended Data Table 2 and Supplementary Table 10). Moreover, in mice extracellular matrix (ECM) genes were overrepresented in some longevity or Nrf2-dependent sets (Supplementary Tables 11 and 12), and *in silico* analysis of longevity-associated genes identified a predicted ECM network[23]. The possible significance of these expression signatures has not been explored.

We investigated the functional importance of specific SKN-1-upregulated *daf-2*(−) collagen genes that decline during ageing, and are upregulated in other longevity-associated gene sets (Extended Data Table 2). SKN-1 increased expression of these genes during adulthood, and delayed their age-related decline in expression in response to multiple interventions that promote longevity: *daf-2* RNAi, rapamycin (mTOR kinase inhibitor[24]), the dietary restriction model *eat-2*, and inhibition of germ cell proliferation (*glp-1*(−))[1] (Fig. 2b–g and Extended Data

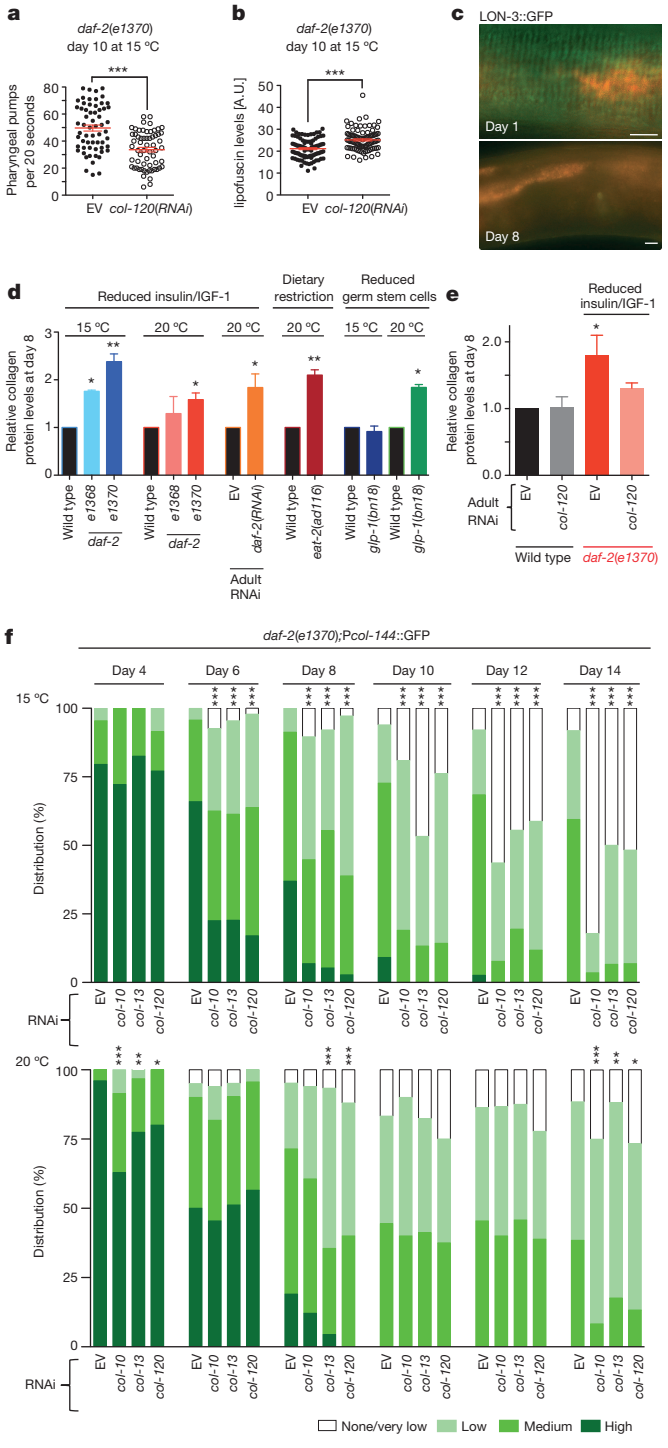

Figure 4 | Importance of ECM remodelling for longevity assurance. **a**, **b**, Adulthood collagen expression is required for rIIS to delay appearance of ageing markers. The same animals were scored in each panel ($N > 60$). Each dot represents an animal; two merged trials; ***$P < 0.0001$ determined with unpaired *t*-test, two-tailed. **c**, Disappearance of the LON-3 collagen from the cuticle during ageing. Typical animals at the indicated days of adulthood are shown. Midsections from representative LON-3::GFP (green fluorescent protein) adults are shown, ventral side down, anterior to the left; scale bar, 10 μm. **d**, Interventions that increase longevity induce adulthood ECM deposition. Total collagen in day 8 adults is indicated by hydroxyproline content. Initiation of *daf-2* RNAi was at day 1. The *glp-1*(*bn18*) mutants were kept at the permissive temperature (15 °C) or shifted to 25 °C until day 1 of adulthood then kept at 20 °C. **e**, Loss of a single collagen interferes with rIIS-induced collagen deposition. In **d**, **e**, $N > 3{,}000$ per sample. Data are mean ± s.e.m. *$P < 0.05$ relative to control, by one sample *t*-test, two-tailed, hypothetical mean of 1. **f**, Dependence of a collagen promoter (*col-144*) on adulthood expression of other SKN-1-upregulated collagens in *daf-2*(*e1370*) under dauer-independent conditions. Scoring is described in Extended Data Fig. 7d. RNAi initiated at day 1 of adulthood had a much more severe effect at 15 °C (upper panel) than 20 °C (lower panel), starting at day 6. $N > 60$ for each condition, one representative trial is shown, with *P* value by χ^2 test (*$P < 0.05$, **$P < 0.001$, ***$P < 0.0001$).

Figs 3i–k and 4a, b). Adulthood knockdown of these collagen genes did not affect wild-type lifespan, but dramatically reduced longevity of the canonical *daf-2* class 2 mutant *e1370* at 15 °C but not 20 °C (Fig. 3a, b, Extended Data Fig. 4c, Extended Data Table 3 and Supplementary Table 13), at which *skn-1* is dispensable for longevity (see above). Additionally, knockdown of these collagens significantly reduced lifespan extension from *daf-2* RNAi at 20 °C, and from other *skn-1*-dependent[14,24,25] longevity interventions (Fig. 3c–e, Extended Data Fig. 4d, Table 3 and Supplementary Table 13). Most of these genes include regions related to other collagens, but *col-120* is unique (Supplementary Table 14), and at 15 °C *daf-2*(*e1370*) but not wild-type lifespan was reduced by the collagen mutation *dpy-1*(*e1*) (Extended Data Fig. 4e and Supplementary Table 13). Lack of a single critical collagen can therefore impair lifespan extension. At 15 °C, *daf-2*(*e1370*) lifespan was also decreased by adulthood knockdown of certain extracellular protease genes from the SKN-1-upregulated *daf-2*(−) set, or other genes important for cuticle formation (Extended Data Fig. 4f and Supplementary Tables 13 and 15). Remarkably, transgenic overexpression of key collagens from the SKN-1-upregulated *daf-2*(−) gene set but not other collagens modestly but consistently increased lifespan (Fig. 3f and Supplementary Table 13). Adulthood SKN-1-dependent expression of particular collagen and ECM genes therefore promotes lifespan extension in diverse pathways that slow *C. elegans* ageing.

Adulthood collagen RNAi did not affect body size, detectably impair cuticle function, or increase markers of various stresses (Extended Data Figs 5a–v and 6a–i). Collagen RNAi sensitized to exogenous oxidative stress, however, and increased the prominence of ageing markers in *daf-2* mutants at 15 °C, and in rapamycin-treated animals (Fig. 4a, b, Extended Data Fig. 6j–m and Supplementary Table 16). Apparently, knockdown of these collagens interfered with the capacity of these interventions to delay ageing.

ECM gene upregulation might allow ECM remodelling to occur in adults. During ageing the collagens LON-3 and ROL-6 decline in expression[22] and largely disappear from the cuticle (Fig. 4c and Extended Data Figs 4a and 7a), indicating that *C. elegans* ECM proteins turn over. Adulthood *daf-2* RNAi and other anti-ageing interventions increased total collagen in older *C. elegans* (Fig. 4d), indicating deposition of new ECM. This also occurred in *daf-2*(*e1370*) (class 2) at 20 °C, even though by adulthood day 8 expression of SKN-1 upregulated *daf-2*(−) collagens was not generally maintained in older *daf-2*(*e1370*) adults under these conditions (Fig. 4d and Extended Data Fig. 7b, c). Perhaps different genes might promote ECM remodelling under dauer-predisposed conditions, consistent with dauers having a distinct cuticle structure (Supplementary Discussion).

Longevity interventions delay ageing by acting through non-cell-autonomous signalling pathways[1]. Adulthood *col-120* knockdown reduced total *daf-2* collagen levels (Fig. 4e), implying that individual collagens and the ECM influence these pathways. Adulthood collagen RNAi also inhibited SKN-1-responsive gene expression in adults that would otherwise be long-lived (Fig. 4f and Extended Data Fig. 7d–g), possibly explaining the importance of these collagens for oxidative stress resistance. These longevity interventions therefore require adulthood expression of particular ECM genes to maintain their beneficial regulatory program. Why would diverse longevity interventions induce and depend upon ECM remodelling? Under conditions of low nutrient availability, it might be advantageous to allocate resources towards ECM maintenance. The ECM also may directly affect signalling that orchestrates these longevity pathways, consistent with studies in other systems that identified signalling functions of collagens, and critical effects of the ECM on signalling pathways[26–28].

We determined that in adult animals rIIS can activate a longevity program that is distinguished from the dauer developmental pathway by its lack of dauer-like traits, and its dependence upon *skn-1* and SKN-1-dependent collagens (Fig. 1f). Further analyses will determine which rIIS longevity mechanisms are linked to the dauer program, and which are dauer-independent and possibly more broadly involved in pathways that promote longevity. Considerable effort has been devoted to enhancing collagen function to maintain youthful human skin during ageing[29]. By demonstrating that increased collagen expression is a shared feature of multiple conserved longevity pathways, our results suggest strategies for promoting ECM function that may be widely applicable. The long-lived naked mole rat is remarkably cancer resistant, at least in part because it produces a uniquely dense hyaluronan, an ECM component[30]. Our results suggest that functional enhancement of the ECM may be generally important for longevity assurance per se. We speculate that interventions that promote collagen and ECM function systemically are likely to be beneficial in human chronic disease and ageing.

Online Content Methods, along with any additional Extended Data display items and Source Data, are available in the online version of the paper; references unique to these sections appear only in the online paper.

Received 14 October 2013; accepted 27 October 2014.
Published online 15 December 2014.

1. Kenyon, C. J. The genetics of ageing. *Nature* **464,** 504–512 (2010).
2. Shore, D. E. & Ruvkun, G. A cytoprotective perspective on longevity regulation. *Trends Cell Biol.* **23,** 409–420 (2013).
3. Lopez-Otin, C., Blasco, M. A., Partridge, L., Serrano, M. & Kroemer, G. The hallmarks of aging. *Cell* **153,** 1194–1217 (2013).
4. Flurkey, K., Papaconstantinou, J., Miller, R. A. & Harrison, D. E. Lifespan extension and delayed immune and collagen aging in mutant mice with defects in growth hormone production. *Proc. Natl Acad. Sci. USA* **98,** 6736–6741 (2001).
5. Wilkinson, J. E. *et al.* Rapamycin slows aging in mice. *Aging Cell* **11,** 675–682 (2012).
6. Myllyharju, J. & Kivirikko, K. I. Collagens, modifying enzymes and their mutations in humans, flies and worms. *Trends Genet.* **20,** 33–43 (2004).
7. Toyama, B. H. & Hetzer, M. W. Protein homeostasis: live long, won't prosper. *Nature Rev. Mol. Cell Biol.* **14,** 55–61 (2013).
8. Partridge, L. & Harvey, P. H. Gerontology. Methuselah among nematodes. *Nature* **366,** 404–405 (1993).
9. McElwee, J. J., Schuster, E., Blanc, E., Thomas, J. H. & Gems, D. Shared transcriptional signature in *Caenorhabditis elegans* dauer larvae and long-lived *daf-2* mutants implicates detoxification system in longevity assurance. *J. Biol. Chem.* **279,** 44533–44543 (2004).
10. Gems, D. *et al.* Two pleiotropic classes of *daf-2* mutation affect larval arrest, adult behavior, reproduction and longevity in *Caenorhabditis elegans*. *Genetics* **150,** 129–155 (1998).
11. Arantes-Oliveira, N., Berman, J. R. & Kenyon, C. Healthy animals with extreme longevity. *Science* **302,** 611 (2003).
12. Sykiotis, G. P. & Bohmann, D. Stress-activated cap'n'collar transcription factors in aging and human disease. *Sci. Signal* **3,** re3 (2010).
13. Tullet, J. M. *et al.* Direct inhibition of the longevity-promoting factor SKN-1 by insulin-like signaling in *C. elegans*. *Cell* **132,** 1025–1038 (2008).
14. Robida-Stubbs, S. *et al.* TOR signaling and rapamycin influence longevity by regulating SKN-1/Nrf and DAF-16/FoxO. *Cell Metab.* **15,** 713–724 (2012).
15. Libina, N., Berman, J. R. & Kenyon, C. Tissue-specific activities of *C. elegans* DAF-16 in the regulation of lifespan. *Cell* **115,** 489–502 (2003).
16. Wolkow, C. A., Kimura, K. D., Lee, M. S. & Ruvkun, G. Regulation of *C. elegans* life-span by insulinlike signaling in the nervous system. *Science* **290,** 147–150 (2000).
17. Narasimhan, S. D. *et al.* PDP-1 links the TGF-β and IIS pathways to regulate longevity, development, and metabolism. *PLoS Genet.* **7,** e1001377 (2011).
18. Oliveira, R. P., Porter Abate, J. & Dilks, K. *et al.* Condition-adapted stress and longevity gene regulation by *Caenorhabditis elegans* SKN-1/Nrf. *Aging Cell* **8,** 524–541 (2009).
19. Pang, S., Lynn, D. A., Lo, J. Y., Paek, J. & Curran, S. P. SKN-1 and Nrf2 couples proline catabolism with lipid metabolism during nutrient deprivation. *Nature Commun.* **5,** 5048 (2014).
20. Herndon, L. A. *et al.* Stochastic and genetic factors influence tissue-specific decline in ageing *C. elegans*. *Nature* **419,** 808–814 (2002).
21. Varani, J. *et al.* Decreased collagen production in chronologically aged skin: roles of age-dependent alteration in fibroblast function and defective mechanical stimulation. *Am. J. Pathol.* **168,** 1861–1868 (2006).
22. Budovskaya, Y. V. *et al.* An elt-3/elt-5/elt-6 GATA transcription circuit guides aging in *C. elegans*. *Cell* **134,** 291–303 (2008).
23. Argmann, C. *et al.* Pparγ2 is a key driver of longevity in the mouse. *PLoS Genet.* **5,** e1000752 (2009).
24. Johnson, S. C., Rabinovitch, P. S. & Kaeberlein, M. mTOR is a key modulator of ageing and age-related disease. *Nature* **493,** 338–345 (2013).
25. Vilchez, D. *et al.* RPN-6 determines *C. elegans* longevity under proteotoxic stress conditions. *Nature* **489,** 263–268 (2012).
26. Seeger-Nukpezah, T. & Golemis, E. A. The extracellular matrix and ciliary signaling. *Curr. Opin. Cell Biol.* **24,** 652–661 (2012).
27. Munger, J. S. & Sheppard, D. Cross talk among TGF-β signaling pathways, integrins, and the extracellular matrix. *Cold Spring Harb. Perspect. Biol.* **3,** a005017 (2011).
28. Fu, H. L. *et al.* Discoidin domain receptors: unique receptor tyrosine kinases in collagen-mediated signaling. *J. Biol. Chem.* **288,** 7430–7437 (2013).

29. Baumann, L. Skin ageing and its treatment. *J. Pathol.* **211,** 241–251 (2007).
30. Tian, X. *et al.* High-molecular-mass hyaluronan mediates the cancer resistance of the naked mole rat. *Nature* **499,** 346–349 (2013).

Supplementary Information is available in the online version of the paper.

Acknowledgements We thank C. Kenyon, S. Mitani, and J. Shim for strains, P. Sengupta for dauer pheromone, C. Obieglo, L. Moronetti, M. Bland, and K. Patel for assistance, and J. Apfeld, E. Greer, C. Kenyon, W. Mair, and Blackwell laboratory members for discussions or comments on the manuscript. Some strains were provided by the Caenorhabditis Genetics Center, which is funded by the National Institutes of Health Office of Research Infrastructure Programs (P40 OD010440). The work was supported by funding from the National Institutes of Health to T.K.B. (GM062891), C.T.M. (New Innovator), and J.P.A. (5T32DK007260), a Diabetes Research Center award to the Joslin Diabetes Center (P30DK036836), and fellowships from the National Science Foundation to J.N.L., and the Swiss National Science Foundation (PBSKP3_140135) to C.Y.E.

Author Contributions All authors participated in designing the experiments, and analysing and interpreting the data. J.N.L. and J.P.A. obtained samples for microarray analysis, performed the microarray experiments, analysed the expression profiling data, and performed the lifespan studies in Extended Data Fig. 2f–h and Supplementary Table 4. C.Y.E. performed all other experiments. C.Y.E. and T.K.B. wrote the manuscript in consultation with the other authors.

Author Information Reprints and permissions information is available at www.nature.com/reprints. The authors declare no competing financial interests. Readers are welcome to comment on the online version of the paper. Correspondence and requests for materials should be addressed to T.K.B. (keith.blackwell@joslin.harvard.edu) or C.T.M. (ctmurphy@princeton.edu).

METHODS

Strains. *C. elegans* strains were maintained on NGM plates and OP50 *Escherichia coli* bacteria at 20 °C as described[31], except that *daf-2* mutants (and corresponding controls for a given assay) were maintained at 15 °C unless otherwise noted. The wild-type strain was N2 Bristol[31]. Mutant strains used are described in Wormbase (www.wormbase.org). LGI: *daf-16*(*mgDf47*, *mu86*); LGII: *eat-2*(*ad1116*); LGIII: *daf-2*(*e1368*, *e1370*, and *m596*), *rrf-3*(*pk1462*), *glp-1*(*bn18*); and LGIV: *eri-1*(*mg366*), *skn-1*(*tm3411*, *zu67*, *zu129*, and *zu135*). LGX: *lin-15B*(*n744*). The following transgenic lines were used: *jgIs5* [ROL- 6::GFP;TTX-3::GFP][32], BC12533 *dpy-5*(*e907*); *sEx12533* [P*col-89*::GFP; *dpy-5*(+)][33], CF1660 *daf-16*(*mu86*); *daf-2*(*e1370*); *muIs84* [P*sod-3*::GFP; pRF4 *rol-6*(*su1006gf*)]; *muEx211* [P*ges-1*::DAF-16::GFP; pRF4 *rol-6*(*su1006gf*)][15], CL2166 *dvIs19* [P*gst-4*::GFP; pRF4 *rol-6*(*su1006gf*)][34], EE86 *mup-4*(*mg36*); *upIs1* [MUP-4::GFP; pRF4 *rol-6*(*su1006gf*)][35], HT1883 *daf-16*(*mgDf50*); *daf-2*(*e1370*) *unc-119*(*ed3*); *lpIs14* [P*daf-16*::DAF-16f::GFP + *unc-119*(+)][36], IG274 *frIs7* [P*col-12*::DsRed; P*nlp-29*::GFP][37], LD001 *ldIs007* [P*skn-1*::SKN-1b/c::GFP; pRF4 *rol-6*(*su1006gf*)][38], MH2051 *kuIs55* [LON-3::GFP; *unc-119*(+)][39], SJ4005 *zcIs4* [Phsp-4::GFP; *lin-15*(+)][40], SJ4103 *zcIs14* [myo-3::GFP(mit)][41], TB1682 *chEx1682* [QUA-1::GFP; pRF4 *rol-6*(*su1006gf*)][42], TJ356 *zIs356* [P*daf-16*::DAF-16a/b::GFP; pRF4 *rol-6*(*su1006gf*)][43], TP12 *kaIs12* [COL-19::GFP][44].

Construction of transgenic lines. To construct the collagen overexpression transgenes, the genomic region of each gene, including approximately 3 kilobases (kb) of promoter, the coding region, and 3′ untranslated region sequences that encompass at least two predicted cleavage/polyadenylation sites, were amplified by PCR. These PCR products were injected at 50 ng μl^{-1} together with 100 ng μl^{-1} of pRF4 *rol-6*(*su1006gf*) into wild-type (N2) animals. For the triple collagen gene transgenic line (*ldEx111*), 50 ng μl^{-1} each of PCR products for *col-10*, *col-13*, *col-120* were injected together with 50 ng μl^{-1} of pRF4 *rol-6*(*su1006gf*). For the control line (*ldEx102*), pBluescript KS(+) 50 ng μl^{-1} was injected along with 100 ng μl^{-1} of pRF4 *rol-6*(*su1006gf*). Lines were isolated from at least two independent transgenic P0 animals. For *col-10*, a 4.4 kb genomic region was amplified using the primers 5′-CCACCAACAACTCCATCCACC-3′ and 5′-GTAAAGTGGGCAGGCCGTAG-3′. The resulting transgenic lines were *ldEx103* and *ldEx104*. For *col-13*, a 4.3 kb genomic region was amplified using the primers 5′-TAGCCCAAGTCTGACCGAAG-3′ and 5′-CGGATCTTCCCAACCAGGAG-3′. The resulting transgenic lines were *ldEx105*, *ldEx106*, *ldEx107*, and *ldEx108*. For *col-120*, a 4.4 kb genomic region was amplified using the primers 5′-CAATATGACCCGAGGCGCTG-3′ and 5′-CGCCAGAATCGTAAGGCTCC-3′. The resulting transgenic lines were: *ldEx109* and *ldEx110*. Transgene overexpression levels were determined by qPCR of 1-day-old adults.

Scoring of phenotypic experiments. No statistical methods were used in choosing sample sizes. In analyses of fluorescent reporters, either all or representative trials were scored blindly. All other phenotypic assays were not scored blindly.

Body length measurements. Animals were maintained at 15 °C and either kept at 15 °C, or shifted to 25 °C at the first day of adulthood. At day 3 of adulthood, animals were mounted on 2% agar pads, immobilized with 0.06% tetramisole and images were taken at ×10 magnification with a Zeiss Axioskop 2 microscope and a Zeiss AxioCam HRc digital camera. Body lengths were measured by placing a line through the middle of the body starting from head to tail using Zeiss AxioVision version 4.8.2.0 (Extended Data Fig. 1d).

Lifespan assays. Strains were age-synchronized by picking larval stage 4 (L4) animals onto fresh OP50 plates, then day 1 adults were placed on either OP50 or RNAi plates containing 50 μM 5-fluoro-2′deoxyuridine (FUdR), unless otherwise indicated, and assayed either at 15, 20, or 25 °C as described in ref. 14. All lifespans were plotted with L4 as time-point = 0. For *glp-1*(*bn18*) lifespans, wild type (N2) and *glp-1*(*bn18*) were maintained at 15 °C, then shifted to 25 °C at the mid-L1 stage as described in ref. 45. At the first day of adulthood they were placed on plates containing FUdR and RNAi bacteria for lifespan assay at 20 °C (Fig. 4g and Extended Data Table 3). For rapamycin lifespans, 1-day-old animals were placed on plates containing FUdR, RNAi bacteria, and either rapamycin (100 μM) dissolved in 0.2% dimethylsulphoxide (DMSO) or 0.2% DMSO control as described in ref. 14. Lifespan was determined at 20 °C (Fig. 3d, Extended Data Table 3 and Supplementary Table 13). For dauer pheromone experiments, day 1 adults were placed on plates containing FUdR, RNAi bacteria, and either crude dauer pheromone (a gift from P. Sengupta) dissolved in 6% ethanol, or 6% ethanol control as described in ref. 46. Those lifespans were determined at 25 °C (Fig. 1e, Extended Data Table 1 and Supplementary Table 2). Animals were classified as dead if they failed to respond to prodding. Exploded or bagged animals were excluded from the statistics. The estimates of survival functions were calculated using the product-limit (Kaplan–Meier) method. The log-rank (Mantel–Cox) method was used to test the null hypothesis and calculate *P* values (JMP software version 9.0.2.).

Scoring of transgenic protein nuclear accumulation or expression. Nuclear accumulation of SKN-1 that was expressed from the *SKN-1bc::GFP* transgene (LD001 strain), which encodes two of the three SKN-1 isoforms, was scored blindly after mounting on slides essentially as in ref. 14 (Extended Data Fig. 1k–n). Scoring was as follows: none, no GFP observed in nuclei; low, some nuclei showed GFP; medium, more than half of the nuclei showed GFP; high, all intestinal nuclei showed GFP. Nuclear accumulation of DAF-16a/b::GFP (*zIs356*) was scored as described in ref. 47 (Extended Data Fig. 1n). Nuclear accumulation of DAF-16f::GFP (*lpIs14*) was scored as follows: none, no GFP observed in nuclei; medium, more than half of the nuclei showed GFP; high, all intestinal nuclei showed GFP (Extended Data Fig. 1o). For P*col-12*::dsRED, P*col-144*::GFP, P*gst-4*::GFP, and P*hsp-4*::GFP, one-day adult animals were placed on RNAi and 3 and/or 7 days later the green or red fluorescence intensity was scored by using a Zeiss AxioSKOP2 microscope. Green or red fluorescence was categorized in none/very low, low, medium, or high intensity and was scored blindly (Fig. 4f and Extended Data Figs 3j–k, 6h–j and 7d–g).

RNAi. RNAi clones were picked from the Ahringer[48] or Vidal[49] libraries. Cultures were grown overnight in lysogeny broth with 12.5 μg ml^{-1} tetracycline and 100 μg ml^{-1} ampicillin, diluted to an attenuance ($D_{600\,nm}$) of 1, and induced with 1 mM IPTG. This culture was seeded onto NGM agar plates containing tetracycline, ampicillin, and additional IPTG. Empty vector plasmid pL4440 was used as control. For double RNAi, clones were grown separately in parallel and after spin-down equal amounts of two clones were mixed and spread on plates.

RNA isolation for microarray analysis. After a timed egg-lay on HT115 *E. coli*, *daf-2*(*e1368*) and *daf-2*(*e1368*); *skn-1*(*zu67*) or *daf-2*(*e1370*) and *daf-2*(*e1370*); *skn-1*(*zu67*) worms were grown at 15 °C until the late L4 stage. Approximately 200 worms were collected and washed three times in M9 buffer[31] to remove bacteria. TriReagent (Sigma) was added, and samples were snap frozen in liquid nitrogen. Total RNA was isolated using TriReagent and an RNA purification column (RNAeasy, Qiagen). RNA quality was determined by visualization of 28S and 18S ribosomal RNA bands on a denaturing formaldehyde gel, or an RNase-free 1.5–2% agarose TBE gel.

RNA preparation, hybridization and data collection for microarray experiments. RNA (325 ng) was linearly amplified and labelled using the Agilent Low RNA Input Linear Amplification Kit, with Cy3- or Cy5-CTP (Perkin Elmer), then RNA copies were hybridized on Agilent 4×44k *C. elegans* arrays. A dye swap replicate was performed for each set of biological replicate samples as previously described[18]. Data were extracted with Agilent Feature Extraction software and submitted to the Princeton University Microarray Database (PUMAdb) for storage and filtering (https://puma.princeton.edu). These microarray data are publicly available at PUMAdb.

Microarray analysis. Data were filtered to remove spots that were not above background intensity in both channels, and replicate spots within each array were averaged. Genes for which more than 20% of data were missing across replicates were removed from further analysis. One-class SAM analysis was used to identify genes that were significantly up- or downregulated across all replicates in a set[50]. Expression profiles were clustered using Cluster 3.0 (ref. 51) and visualized using Java TreeView[52]. Up- and downregulated genes identified by SAM analysis were submitted to DAVID[53] to identify overrepresented functional annotations. Annotations used were Gene Ontology (GO) Biological Process FAT (GO BP, filtered by DAVID to remove the broadest GO terms), GO Molecular Function, Kegg Pathway, and Interpro Protein Domains. The Benjamini test for multiple hypothesis testing was applied to *P* values. Up- and downregulated genes were also submitted to GOToolBox to perform a hypergeometric test using the Benjamini–Hochberg correction. Enriched GO terms were submitted to ReviGO to remove redundant terms. Co-occurrence between our data sets and previously published data sets was visualized with GeneVenn[54] and BioInfoRx Area-Proportional Venn Diagram.

Motif analysis. We used two distinct algorithms, Weeder[55] and FIRE[56], to perform an unbiased search for overrepresented sequences in the promoters of SKN-1-regulated genes that were identified by SAM. We submitted upstream sequences (1,000 base pairs (bp)) to Weeder and performed a scan for motifs of length 6 and 8 ('normal' scan mode). FIRE was run using default parameters, with all genes partitioned into three groups to identify motifs that were informative about each group: SKN-1-upregulated, SKN-1-downregulated, and background. To search in a directed manner for occurrence of the consensus SKN-1 binding motif, we used RSATools[57] to search the 600 bp upstream of up- and downregulated targets for the SKN-1 binding motif (WWTRTCAT). For comparison with the percentage of promoters in a random sample of genes that would be expected to contain the SKN-1 motif, we searched for the motif in 10,000 random samplings of gene promoter sets of equal size to the number of up- or downregulated genes, to determine a distribution empirically. To calculate a *P* value, we *z*-transformed the percentage of SKN-1 target promoters ($z = (\%_{SKN\text{-}1} - \mu)/\sigma$), where μ and σ are the mean and standard deviation of the distribution.

qPCR assays. For validation of the microarray data with *skn-1* and *daf-16* mutants, *C. elegans* were allowed to lay eggs for 3–4 h on RNAi plates. After 2–4 days (depending upon the temperature and strain), 200 L4 worms were harvested (15 °C for Extended Data Fig. 2c; 20 °C Extended Data Fig. 2m–t). For adult RNAi, 1-day-old adults were placed on RNAi plates and 3–8 days later 100–200 worms were

harvested (Fig. 2a–c and Extended Data Fig. 4b). For rapamycin treatment, 1-day-old animals were placed on plates containing rapamycin (100 μM) dissolved in 0.2% DMSO or in 0.2% DMSO control as described in ref. 14 and 3 days later mRNA was harvested for qPCR (Extended Data Fig. 3l–m). For the *glp-1* experiment, *glp-1*(*bn18*) or wild-type (N2) animals were maintained at 15 °C and L2 worms were upshifted to 25 °C. Day 1 adults were placed on L4440 (empty vector RNAi) plates at 20 °C and 3 days later 200 worms were harvested (Extended Data Fig. 3p–q). RNA was isolated with Trizol (TRI REAGENT Sigma), DNase-treated, and cleaned over a column (RNA Clean & Concentrator™ ZYMO Research). First-strand complementary DNA (cDNA) was synthesized in duplicate from each sample (Invitrogen SuperScript III). SYBR green was used to perform qPCR (ABI 7900). For each primer set, a standard curve from genomic DNA accompanied the duplicate cDNA samples[58]. mRNA levels relative to N2 control were determined by normalizing to the number of worms and the geometric mean of three reference genes (*cdc-42*, *pmp-3*, and Y45F10D.4 (ref. 59)). Primer sequences are listed in Supplementary Table 17. Except for *col-12/13*, primers bound uniquely to the corresponding gene transcript (Supplementary Tables 14 and 17). At least two biological replicates were examined for each sample. For statistical analysis, one sample *t*-test, two-tailed, hypothetical mean of 1, was used for comparison using Prism 4.0a software (GraphPad).

Oxidative stress assays. In oxidative stress assays, day 1 *daf-2* or *skn-1* adults were placed in 5 mM sodium arsenite (in 1 ml H_2O) at 20 °C and scored for survival hourly (Supplementary Table 7). For RNAi oxidative stress assays, wild-type (N2) or *daf-2*(*e1370*) day 1 adults were placed on RNAi plates at 15 °C, and 3 days later animals were placed either on plates containing 15.4 mM t-BOOH and scored hourly at 20 °C, or in 5 mM sodium arsenite (in 1 ml M9 buffer) and scored after 21 h (N2) or 30 h (*daf-2*) at 20 °C (Extended Data Fig. 6j–l and Supplementary Table 16).

Age-related phenotypic marker and body-size assays. Age-related phenotypes were described in ref. 60. One-day-old animals were placed on RNAi food until day 10 of adulthood and the following phenotypes were scored. (1) Pharyngeal pumping was determined by counting grinder movements in 20 s intervals when the animals were placed on food (Fig. 4a and Extended Data Fig. 6m). (2) Lipofuscin levels were determined by mounting animals onto slides and taking bright-field and 4′,6-diamidino-2-phenylindole (DAPI) channel pictures with a Zeiss Imager M2 microscope. Blue fluorescence from the DAPI channel pictures were analysed in Image J (http://imagej.nih.gov/ij/) by selecting the intestine and measuring the mean grey value minus the background (Fig. 4b). (3) The body size was determined from bright-field images by drawing a line through the middle of the worm from anterior to posterior by using Zeiss Zen 2012 software (Extended Data Fig. 6a).

Collagen assays. Synchronized L1 larvae were placed on 10 cm NGM plates containing OP50 bacteria at 15, 20, or 25 °C and monitored for development to the L4 stage. After an additional day, day 1 adults were either harvested for the assay (Extended Data Fig. 7b), or placed on either 10 cm OP50 or RNAi plates containing 50 μM FUdR and maintained at the corresponding temperature. At day 8 of adulthood, the remaining animals were harvested (Fig. 4d, e). In each case, the animals were washed three times with M9, the number of worms was determined, and at least 3,000 worms per strain and condition were used for the assay. Collagen levels were determined using the QuickZyme Biosciences Total Collagen Kit (QZBTOT COL1), which detects hydroxyproline[61], according to the manufacturer's instructions.

Barrier function assay. One-day-old adults were placed on RNAi food and at day 9 were harvested, washed three times with M9 and incubated in 1 μg ml^{-1} Hoechst (Hoechst 33342, which is cuticle-impermeable but membrane-permeable) for 15 min in darkness at room temperature (22 °C). The animals were then washed three times in M9, allowed to recover for 10 min on plates with food, and mounted for microscopy (Extended Data Fig. 6b, c; method adapted from ref. 62).

31. Brenner, S. The genetics of *Caenorhabditis elegans*. *Genetics* **77,** 71–94 (1974).
32. Kim, T. H. *et al.* Tyrosylprotein sulfotransferase regulates collagen secretion in *Caenorhabditis elegans*. *Mol. Cells* **29,** 413–418 (2010).
33. McKay, S. J. *et al.* Gene expression profiling of cells, tissues, and developmental stages of the nematode *C. elegans*. *Cold Spring Harb. Symp. Quant. Biol.* **68,** 159–169 (2003).
34. Link, C. D. & Johnson, C. J. Reporter transgenes for study of oxidant stress in *Caenorhabditis elegans*. *Methods Enzymol.* **353,** 497–505 (2002).
35. Hong, L. *et al.* MUP-4 is a novel transmembrane protein with functions in epithelial cell adhesion in *Caenorhabditis elegans*. *J. Cell Biol.* **154,** 403–414 (2001).
36. Kwon, E. S., Narasimhan, S. D., Yen, K. & Tissenbaum, H. A. A new DAF-16 isoform regulates longevity. *Nature* **466,** 498–502 (2010).
37. Pujol, N. *et al.* Distinct innate immune responses to infection and wounding in the *C. elegans* epidermis. *Curr. Biol.* **18,** 481–489 (2008).
38. An, J. H. & Blackwell, T. K. SKN-1 links *C. elegans* mesendodermal specification to a conserved oxidative stress response. *Genes Dev.* **17,** 1882–1893 (2003).
39. Suzuki, Y., Morris, G. A., Han, M. & Wood, W. B. A cuticle collagen encoded by the *lon-3* gene may be a target of TGF-β signaling in determining *Caenorhabditis elegans* body shape. *Genetics* **162,** 1631–1639 (2002).
40. Calfon, M. *et al.* IRE1 couples endoplasmic reticulum load to secretory capacity by processing the XBP-1 mRNA. *Nature* **415,** 92–96 (2002).
41. Benedetti, C., Haynes, C. M., Yang, Y., Harding, H. P. & Ron, D. Ubiquitin-like protein 5 positively regulates chaperone gene expression in the mitochondrial unfolded protein response. *Genetics* **174,** 229–239 (2006).
42. Hao, L. *et al.* The hedgehog-related gene *qua-1* is required for molting in *Caenorhabditis elegans*. *Dev. Dyn.* **235,** 1469–1481 (2006).
43. Henderson, S. T. & Johnson, T. E. *daf-16* integrates developmental and environmental inputs to mediate aging in the nematode *Caenorhabditis elegans*. *Curr. Biol.* **11,** 1975–1980 (2001).
44. Thein, M. C. *et al. Caenorhabditis elegans* exoskeleton collagen COL-19: an adult-specific marker for collagen modification and assembly, and the analysis of organismal morphology. *Dev. Dyn.* **226,** 523–539 (2003).
45. Arantes-Oliveira, N., Apfeld, J., Dillin, A. & Kenyon, C. Regulation of life-span by germ-line stem cells in *Caenorhabditis elegans*. *Science* **295,** 502–505 (2002).
46. Neal, S. J., Kim, K. & Sengupta, P. Quantitative assessment of pheromone-induced dauer formation in *Caenorhabditis elegans*. *Methods Mol. Biol.* **1068,** 273–283 (2013).
47. Curran, S. P. & Ruvkun, G. Lifespan regulation by evolutionarily conserved genes essential for viability. *PLoS Genet.* **3,** e56 (2007).
48. Kamath, R. S., Martinez-Campos, M., Zipperlen, P., Fraser, A. G. & Ahringer, J. Effectiveness of specific RNA-mediated interference through ingested double-stranded RNA in *Caenorhabditis elegans*. *Genome Biol.* **2,** research0002 (2001).
49. Rual, J. F. *et al.* Toward improving *Caenorhabditis elegans* phenome mapping with an ORFeome-based RNAi library. *Genome Res.* **14,** 2162–2168 (2004).
50. Tusher, V. G., Tibshirani, R. & Chu, G. Significance analysis of microarrays applied to the ionizing radiation response. *Proc. Natl Acad. Sci. USA* **98,** 5116–5121 (2001).
51. Eisen, M. B., Spellman, P. T., Brown, P. O. & Botstein, D. Cluster analysis and display of genome-wide expression patterns. *Proc. Natl Acad. Sci. USA* **95,** 14863–14868 (1998).
52. Saldanha, A. J. Java Treeview—extensible visualization of microarray data. *Bioinformatics* **20,** 3246–3248 (2004).
53. Dennis, G. Jr *et al.* DAVID: Database for Annotation, Visualization, and Integrated Discovery. *Genome Biol.* **4,** 3 (2003).
54. Pirooznia, M., Nagarajan, V. & Deng, Y. GeneVenn - a web application for comparing gene lists using Venn diagrams. *Bioinformation* **1,** 420–422 (2007).
55. Pavesi, G., Mereghetti, P., Mauri, G. & Pesole, G. Weeder Web: discovery of transcription factor binding sites in a set of sequences from co-regulated genes. *Nucleic Acids Res.* **32,** W199–W203 (2004).
56. Elemento, O., Slonim, N. & Tavazoie, S. A universal framework for regulatory element discovery across all genomes and data types. *Mol. Cell* **28,** 337–350 (2007).
57. Thomas-Chollier, M. *et al.* RSAT: regulatory sequence analysis tools. *Nucleic Acids Res.* **36,** W119–W127 (2008).
58. Glover-Cutter, K., Kim, S., Espinosa, J. & Bentley, D. L. RNA polymerase II pauses and associates with pre-mRNA processing factors at both ends of genes. *Nature Struct. Mol. Biol.* **15,** 71–78 (2008).
59. Hoogewijs, D., Houthoofd, K., Matthijssens, F., Vandesompele, J. & Vanfleteren, J. R. Selection and validation of a set of reliable reference genes for quantitative sod gene expression analysis in *C. elegans*. *BMC Mol. Biol.* **9,** 9 (2008).
60. Huang, C., Xiong, C. & Kornfeld, K. Measurements of age-related changes of physiological processes that predict lifespan of *Caenorhabditis elegans*. *Proc. Natl Acad. Sci. USA* **101,** 8084–8089 (2004).
61. Zito, E., Hansen, H. G., Yeo, G. S., Fujii, J. & Ron, D. Endoplasmic reticulum thiol oxidase deficiency leads to ascorbic acid depletion and noncanonical scurvy in mice. *Mol. Cell* **48,** 39–51 (2012).
62. Kage-Nakadai, E. *et al.* Two very long chain fatty acid acyl-CoA synthetase genes, *acs-20* and *acs-22*, have roles in the cuticle surface barrier in *Caenorhabditis elegans*. *PLoS ONE* **5,** e8857 (2010).
63. Hertweck, M., Gobel, C. & Baumeister, R. C. *elegans* SGK-1 is the critical component in the Akt/PKB kinase complex to control stress response and life span. *Dev. Cell* **6,** 577–588 (2004).
64. Patel, D. S. *et al.* Clustering of genetically defined allele classes in the *Caenorhabditis elegans* DAF-2 insulin/IGF-1 receptor. *Genetics* **178,** 931–946 (2008).
65. Dillin, A., Crawford, D. K. & Kenyon, C. Timing requirements for insulin/IGF-1 signaling in *C. elegans*. *Science* **298,** 830–834 (2002).
66. Apfeld, J. & Kenyon, C. Cell nonautonomy of *C. elegans daf-2* function in the regulation of diapause and life span. *Cell* **95,** 199–210 (1998).
67. Timmons, L., Tabara, H., Mello, C. C. & Fire, A. Z. Inducible systemic RNA silencing in *Caenorhabditis elegans*. *Mol. Biol. Cell* **14,** 2972–2983 (2003).
68. Kennedy, S., Wang, D. & Ruvkun, G. A conserved siRNA-degrading RNase negatively regulates RNA interference in *C. elegans*. *Nature* **427,** 645–649 (2004).
69. Blackwell, T. K., Bowerman, B., Priess, J. R. & Weintraub, H. Formation of a monomeric DNA binding domain by Skn-1 bZIP and homeodomain elements. *Science* **266,** 621–628 (1994).
70. Niu, W. *et al.* Diverse transcription factor binding features revealed by genome-wide ChIP-seq in *C. elegans*. *Genome Res.* **21,** 245–254 (2011).
71. Simmer, F. *et al.* Loss of the putative RNA-directed RNA polymerase RRF-3 makes *C. elegans* hypersensitive to RNAi. *Curr. Biol.* **12,** 1317–1319 (2002).
72. Jones, S. J. *et al.* Changes in gene expression associated with developmental arrest and longevity in *Caenorhabditis elegans*. *Genome Res.* **11,** 1346–1352 (2001).
73. Hillier, L. W. *et al.* Genomics in *C. elegans*: so many genes, such a little worm. *Genome Res.* **15,** 1651–1660 (2005).
74. Shaw, W. M., Luo, S., Landis, J., Ashraf, J. & Murphy, C. T. The *C. elegans* TGF-β dauer pathway regulates longevity via insulin signaling. *Curr. Biol.* **17,** 1635–1645 (2007).
75. Hedgecock, E. M. & Herman, R. K. The *ncl-1* gene and genetic mosaics of *Caenorhabditis elegans*. *Genetics* **141,** 989–1006 (1995).

76. Schultz, R. D. & Gumienny, T. L. Visualization of *Caenorhabditis elegans* cuticular structures using the lipophilic vital dye DiI. *J. Vis. Exp.* **59,** e3362 (2012).
77. Kim, T. H., Kim, Y. J., Cho, J. W. & Shim, J. A novel zinc-carboxypeptidase SURO-1 regulates cuticle formation and body morphogenesis in *Caenorhabditis elegans*. *FEBS Lett.* **585,** 121–127 (2011).
78. Viswanathan, M., Kim, S. K., Berdichevsky, A. & Guarente, L. A role for SIR-2.1 regulation of ER stress response genes in determining *C. elegans* life span. *Dev. Cell* **9,** 605–615 (2005).
79. Menzel, R. *et al.* The nematode *Caenorhabditis elegans*, stress and aging: identifying the complex interplay of genetic pathways following the treatment with humic substances. *Front. Genet.* **3,** 50 (2012).
80. Pietsch, K. *et al.* Meta-analysis of global transcriptomics suggests that conserved genetic pathways are responsible for quercetin and tannic acid mediated longevity in *C. elegans*. *Front. Genet.* **3,** 48 (2012).
81. Gusarov, I. *et al.* Bacterial nitric oxide extends the lifespan of *C. elegans*. *Cell* **152,** 818–830 (2013).
82. Schmeisser, S. *et al.* Neuronal ROS signaling rather than AMPK/sirtuin-mediated energy sensing links dietary restriction to lifespan extension. *Mol. Metabol.* **2,** 1–11 (2013).
83. Staab, T. A. *et al.* The conserved SKN-1/Nrf2 stress response pathway regulates synaptic function in *Caenorhabditis elegans*. *PLoS Genet.* **9,** e1003354 (2013).
84. Iser, W. B., Wilson, M. A., Wood, W. H., III, Becker, K. & Wolkow, C. A. Co-regulation of the DAF-16 target gene, *cyp-35B1/dod-13*, by HSF-1 in *C. elegans* dauer larvae and *daf-2* insulin pathway mutants. *PLoS ONE* **6,** e17369 (2011).
85. Zarse, K. *et al.* Impaired insulin/IGF1 signaling extends life span by promoting mitochondrial L-proline catabolism to induce a transient ROS signal. *Cell Metab.* **15,** 451–465 (2012).
86. Halaschek-Wiener, J. *et al.* Analysis of long-lived *C. elegans daf-2* mutants using serial analysis of gene expression. *Genome Res.* **15,** 603–615 (2005).
87. Mair, W. *et al.* Lifespan extension induced by AMPK and calcineurin is mediated by CRTC-1 and CREB. *Nature* **470,** 404–408 (2011).
88. Greer, E. L. *et al.* Members of the H3K4 trimethylation complex regulate lifespan in a germline-dependent manner in *C. elegans*. *Nature* **466,** 383–387 (2010).
89. Cristina, D., Cary, M., Lunceford, A., Clarke, C. & Kenyon, C. A regulated response to impaired respiration slows behavioral rates and increases lifespan in *Caenorhabditis elegans*. *PLoS Genet.* **5,** e1000450 (2009).
90. Chen, D. *et al.* Germline signaling mediates the synergistically prolonged longevity produced by double mutations in *daf-2* and *rsks-1* in *C. elegans*. *Cell Rep.* **5,** 1600–1610 (2013).
91. Chen, S. *et al.* The conserved NAD(H)-dependent corepressor CTBP-1 regulates *Caenorhabditis elegans* life span. *Proc. Natl Acad. Sci. USA* **106,** 1496–1501 (2009).
92. Huang da. W., Sherman, B. T. & Lempicki, R. A. Bioinformatics enrichment tools: paths toward the comprehensive functional analysis of large gene lists. *Nucleic Acids Res.* **37,** 1–13 (2009).
93. Huang, da. W., Sherman, B. T. & Lempicki, R. A. Systematic and integrative analysis of large gene lists using DAVID bioinformatics resources. *Nature Protocols* **4,** 44–57 (2009).

a

Genotype	Lifespan extension 15°C	*skn-1*-dependent 15°C	Lifespan extension 20°C	*skn-1*-dependent 20°C	Lifespan extension 25°C	*skn-1*-dependent 25°C	*Dauer entry 25°C	*Class 2 traits 20°C
daf-2(RNAi)	56%	Yes	62%	Yes	64%	Yes	No	No
daf-2(e1368) Class 1	34%	Yes	46%	Partial	ND	ND	Yes	No
daf-2(e1370) Class 2	50%	Yes	53%	No	ND	ND	Yes	Yes
daf-2(e1368) daf-2(RNAi)	193%	Yes	139%	Partial	ND	ND	Yes	No

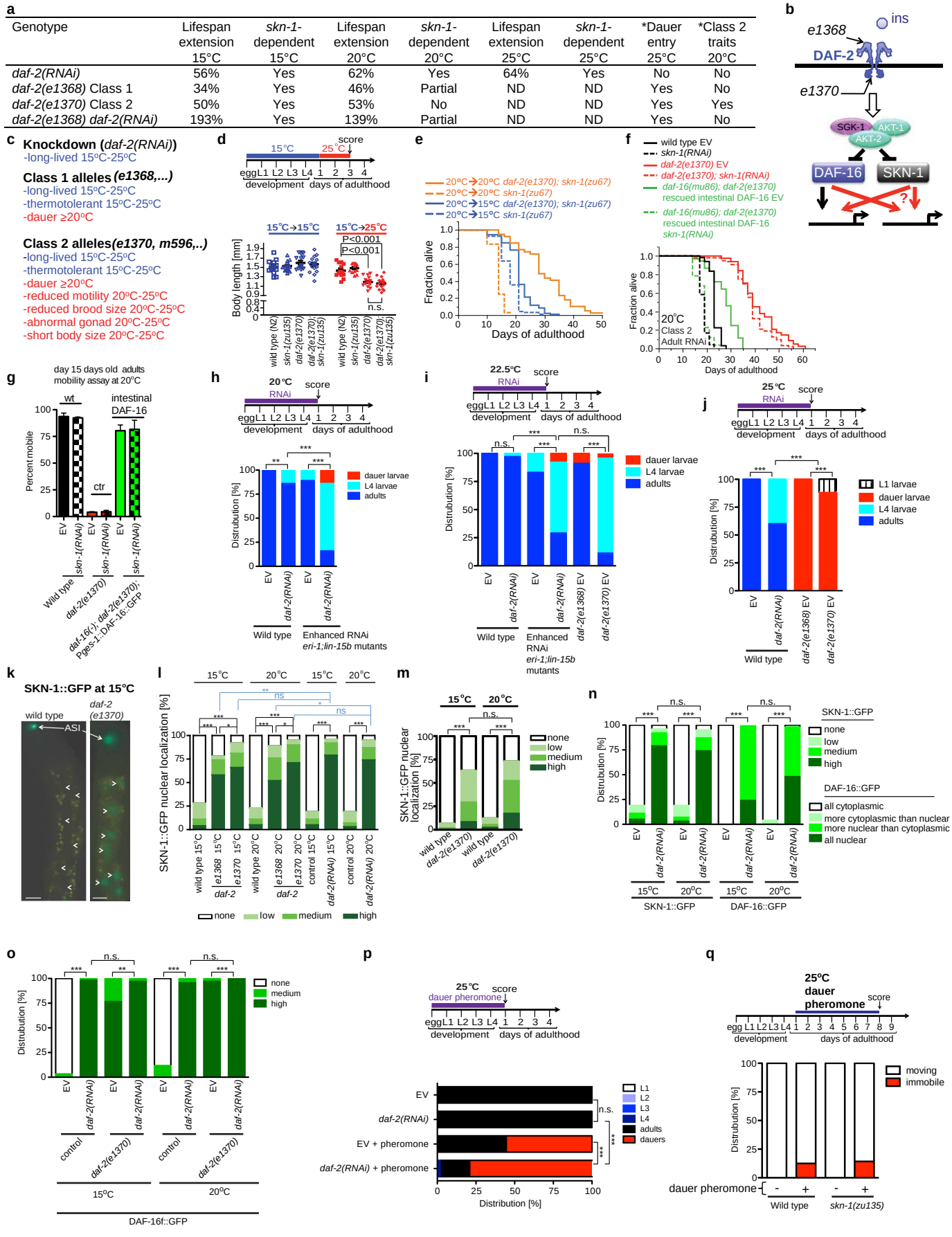

Extended Data Figure 1 | Analyses of rIIS under dauer-independent and dauer-predisposed conditions. **a**, Data from this study illustrating that rIIS longevity dependence upon *skn-1* correlates with low dauer pathway activity, not temperature or percentage increase in mean lifespan extension (*described in the Supplementary Discussion). **b**, Partial schematic of the IIS pathway in *C. elegans*. Insulin-like peptides (ins) bind to DAF-2, leading to activation of the AKT-1/2 and possibly SGK-1 kinases[1,13,63], which phosphorylate DAF-16 and SKN-1. Class 1 *daf-2* mutations are typically located on the extracellular portion of DAF-2, whereas most class 2 mutations affect its intracellular domains[64]. **c**, Mutant phenotypes of *daf-2*. Red indicates penetrance specifically at higher temperatures (Supplementary Discussion). **d**, The class 2 (dauer-related) *daf-2* trait of reduced body length is *skn-1*-independent. Each dot represents an animal, with *P* values determined by one-way analysis of variance (ANOVA) with post hoc Tukey's test. **e**, Dependence of dauer-independent *daf-2* longevity on adulthood *skn-1*. *daf-2*(*e1370*) lifespan extension requires *skn-1* when the temperature is downshifted to 15 °C specifically during adulthood (blue). For additional information see Supplementary Table 2. **f**, The *skn-1* dependence of *daf-2*(*e1370*) longevity at 20 °C when DAF-16 is expressed specifically in the intestine (strain description in Extended Data Table 1). **g**, Intestine-specific DAF-16 expression fails to rescue a class 2 dauer-like trait (immobility) in *daf-2*(*e1370*). **h**–**j**, Condition-specific induction of dauer by *daf-2* RNAi. The *daf-2* RNAi fails to induce dauer entry even at 25 °C (**j**), although some dauers are seen under more extreme conditions (27 °C)[65]. The activity of IIS and DAF-16 in neurons is critical for dauer regulation[15,16,66], and in the wild-type RNAi is comparatively ineffective in neurons[67], suggesting that the extremely weak dauer propensity of *daf-2* RNAi might derive from a failure to reduce IIS sufficiently in neurons. Supporting this idea, *daf-2* RNAi induced dauer entry even at 20 °C in *eri-1*(*mg366*); *lin-15B*(*n744*) mutants, in which neuronal RNAi is robust[68] (**h**). $N > 100$ for each condition, two merged trials. **k**–**n**, Robust SKN-1 and DAF-16 nuclear localization under conditions of dauer inactivity. SKN-1 nuclear accumulation is inhibited comparably by IIS at 15 and 20 °C. SKN-1 is constitutively localized to ASI neuron nuclei in wild-type animals, and accumulates in intestinal nuclei in *daf-2*(*e1370*)[13]. **k**, Extent of IIS reduction from *daf-2*(*e1370*) at 15 °C, indicated by nuclear SKN-1::GFP. Chevrons indicate intestinal nuclei; scale bar, 20 μm. SKN-1::GFP (LD001) in intestinal nuclei is quantified in **l**, **m**. $N > 60$ for each condition and trial, three merged trials with *P* values determined by χ^2 test. Nuclear accumulation was scored as in Methods. **n**, The *daf-2* RNAi comparably induces SKN-1::GFP (LD001) and DAF-16::GFP (TJ356) intestinal nuclear localization at 15 and 20 °C. $N > 60$ for each condition, one trial with all experimental conditions done in parallel. **o**, Comparable nuclear accumulation of DAF-16f::GFP (*lpIs14*) induced by *daf-2* RNAi and *daf-2*(*e1370*) at 15 and 20 °C. $N > 60$ for each condition, one trial performed in parallel. **p**, **q**, Induction of dauer development (**p**) and dauer-like traits (*skn-1*-independent) (**q**) by the crude dauer pheromone preparation used in lifespan assays (Fig. 1e, Extended Data Table 1 and Supplementary Table 2). In **p**, $N > 100$ for each condition, one trial. In **q**, $N = 30$ for each condition, three merged trials. For **h**–**j**, **l**–**o**, *P* values were determined by χ^2 test; n.s., not significant, $*P < 0.05$, $**P < 0.001$, $***P < 0.0001$.

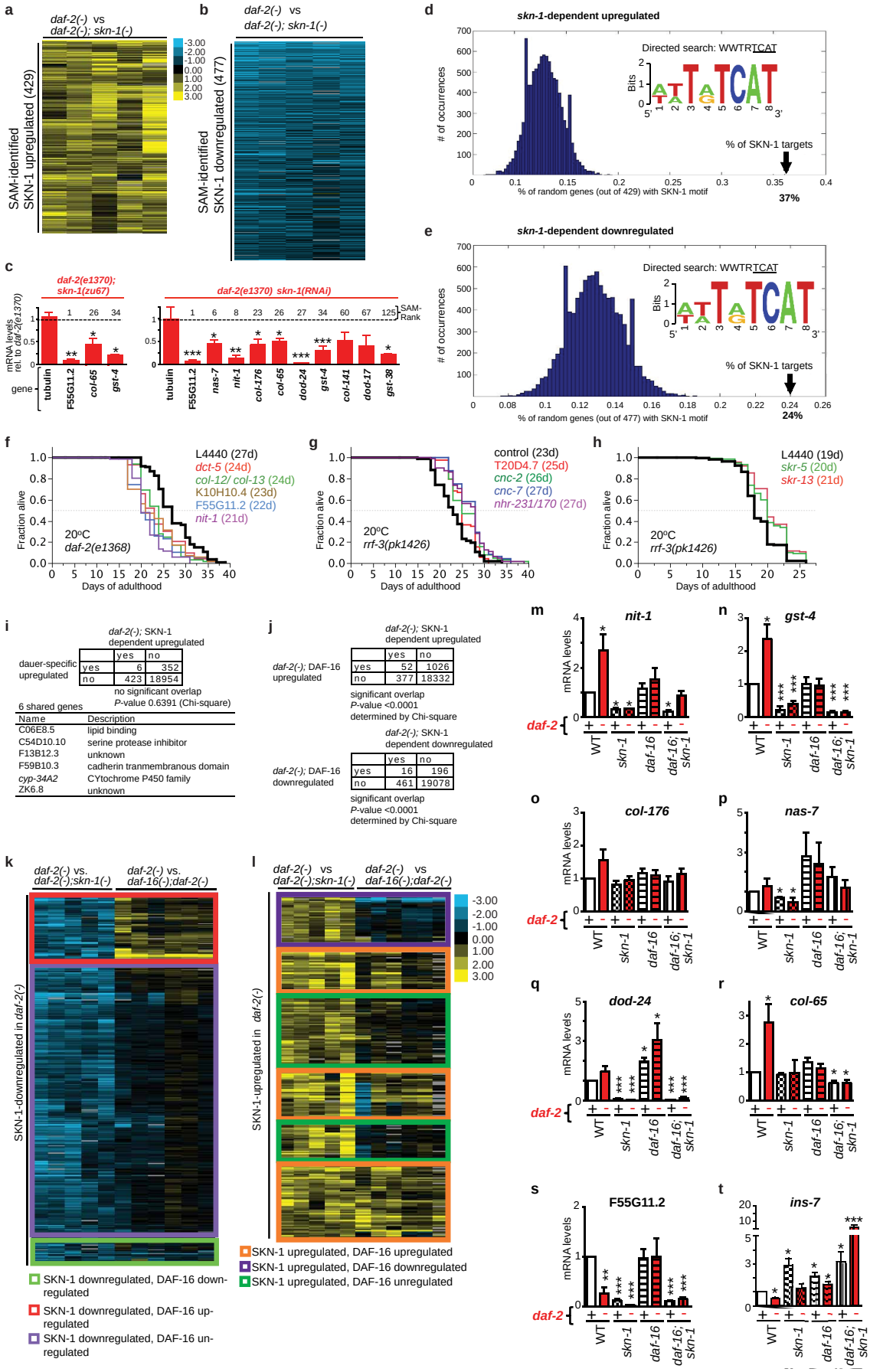

Extended Data Figure 2 | Identification of SKN-1-regulated *daf-2*(−) genes. **a**, Heatmap of 429 genes identified by SAM as significantly upregulated by SKN-1 in *daf-2* mutants. **b**, Four hundred and seventy-seven genes identified by SAM as significantly downregulated by SKN-1 in *daf-2* mutants (Supplementary Table 3). The SKN-1-downregulated *daf-2*(−) set was enriched for genes involved in ubiquitin-mediated proteolysis (E3 ligase/SCF, F-box; Supplementary Table 8). Columns represent biological samples. Blue, down; black, unregulated. **c**, Confirmation of microarray data for SKN-1-upregulated *daf-2*(−) genes by qPCR at 15 °C. One and three biological replicates were analysed in the left and right panels, respectively. SAM scores are in Supplementary Table 3. Data are mean ± s.e.m. $*P < 0.05$, $**P < 0.001$, $***P < 0.0001$ relative to *daf-2*, determined by one sample *t*-test, two-tailed, hypothetical mean of 1. **d**, **e**, Enrichment of SKN-1 binding sites upstream of SKN-1-regulated *daf-2*(−) genes. An unbiased search using the Weeder and FIRE algorithms did not detect any overrepresented form of the consensus SKN-1 binding motif (WWTRTCAT) (W = A/T, R = G/A)[69]. Given the degeneracy of this motif, we used RSATools to perform a directed search of 600 bp upstream of SKN-1 upregulated (**d**) and downregulated (**e**) genes. This search window was based upon the location of SKN-1 binding sites identified by genome-wide chromatin immunoprecipitation followed by sequencing (ChIP-seq) using transgenically expressed SKN-1 (ref. 70). A SKN-1 motif was detected at only 13% of a random sample of 10,000 genes, but at 37% and 24% of the SKN-1-upregulated (out of 429 genes) and downregulated genes (out of 477 genes), respectively. **f**, Importance of SKN-1-upregulated *daf-2*(−) genes for *daf-2*(*e1368*) lifespan. The class 1 *daf-2* allele *e1368* is partly dependent upon *skn-1* for lifespan extension at 20 °C (Extended Data Table 1)[13]. Adult RNAi against 5 of 12 genes tested reduced *daf-2*(*e1368*) lifespan at 20 °C. **g**, **h**, Several SKN-1-downregulated *daf-2*(−) genes decrease lifespan. Knockdown was performed in the RNAi-sensitive strain *rrf-3*(*pk1426*)[71]. **g**, Genes for which RNAi knockdown increased lifespan, from 12 that were analysed without regard to their function. **h**, Analysis of six Skp1-related genes, an overrepresented category among SKN-1-downregulated *daf-2*(−) genes (Supplementary Table 8). Only genes that affected lifespan are shown. Other data and all statistics are in Supplementary Table 6. For 15 other SKN-1-downregulated *daf-2*(−) genes, it has been shown previously that RNAi increases lifespan (Supplementary Table 5). Parts **f** and **g** each show a single trial, and a composite of three trials is shown in **h**. In **g** the negative RNAi control is *elpc-4*(*RNAi*) instead of L4440. Mean lifespan (in days) is indicated for each gene. **i**, Overlap between the *daf-2*(−); SKN-1-dependent upregulated gene set (429 genes, this study) and a set of genes preferentially upregulated in dauers (358 genes)[72]. The overlap of six genes was not significant ($P = 0.6391$ by two-sided χ^2 test). The number of genes that were present in neither set (no/no) was determined by subtracting the total number in both gene sets from the total number of genes encoded in *C. elegans* 19,735 (ref. 73). **j**, Overlaps between SKN-1-regulated *daf-2*(−) and DAF-16-regulated *daf-2*(−) gene sets[74]. For both up- and downregulated *daf-2*(−) genes, overlaps between the SKN-1- and DAF-16-regulated sets were significant ($P < 0.0001$ determined by two-sided χ^2 test). Moreover, hierarchical clustering identified additional SKN-1-upregulated *daf-2*(−) genes that were also upregulated by DAF-16 even though they were not present in this list of highest-confidence DAF-16-regulated genes (**l**). The number of genes that were in neither set (no/no) was determined as in **i**. **k**, Hierarchical clustering of SKN-1-downregulated *daf-2*(−) gene sets with DAF-16-regulated genes. SKN-1-regulated genes identified here were queried as to how they were influenced by DAF-16 in a comparison of *daf-2*(*e1370*) versus *daf-16*(*mu86*); *daf-2*(*e1370*) animals raised at 20 °C (ref. 74). Three hundred and ninety-three SKN-1-upregulated *daf-2*(−) genes that were present in this DAF-16-regulated data set are shown. Most SKN-1-downregulated *daf-2*(−) genes did not appear to be regulated by DAF-16. **l**, Hierarchical clustering of SKN-1-upregulated *daf-2*(−) genes with DAF-16-regulated genes that were identified by comparing *daf-2*(*e1370*) versus *daf-16*(*mu86*); *daf-2*(*e1370*) at 20 °C (ref. 74). Two hundred and seventy-two SKN-1-upregulated *daf-2*(−) genes that were present in this DAF-16-regulated data set are shown, 46% of which were upregulated by both SKN-1 and DAF-16. Yellow, up; blue, down; black, unregulated. **m**–**t**, Effects of SKN-1 and DAF-16 on individual genes in response to *daf-2* RNAi at 20 °C. A qPCR analysis of *skn-1*(*zu67*), *daf-16*(*mgDf47*), and *daf-16*(*mgDf47*); *skn-1*(*zu67*) double mutants indicated that many genes are upregulated by *daf-2*(*RNAi*) (red) in a *skn-1*-dependent manner, but also that these genes vary in how they are affected by DAF-16. DAF-16 and SKN-1 increased activity of *gst-4*, *col-65*, and *col-176*, but DAF-16 seemed to downregulate *dod-24*, *nas-7*, and *F55G11.2*. All of these genes except *ins-7* were identified in our *daf-2*; *skn-1* data sets. For each condition, three biological samples of 200 worms each were analysed by qPCR. All data are mean ± s.e.m. $*P < 0.05$, $**P < 0.001$, $***P < 0.0001$ relative to wild-type RNAi control, determined by one sample *t*-test, two-tailed, hypothetical mean of 1.

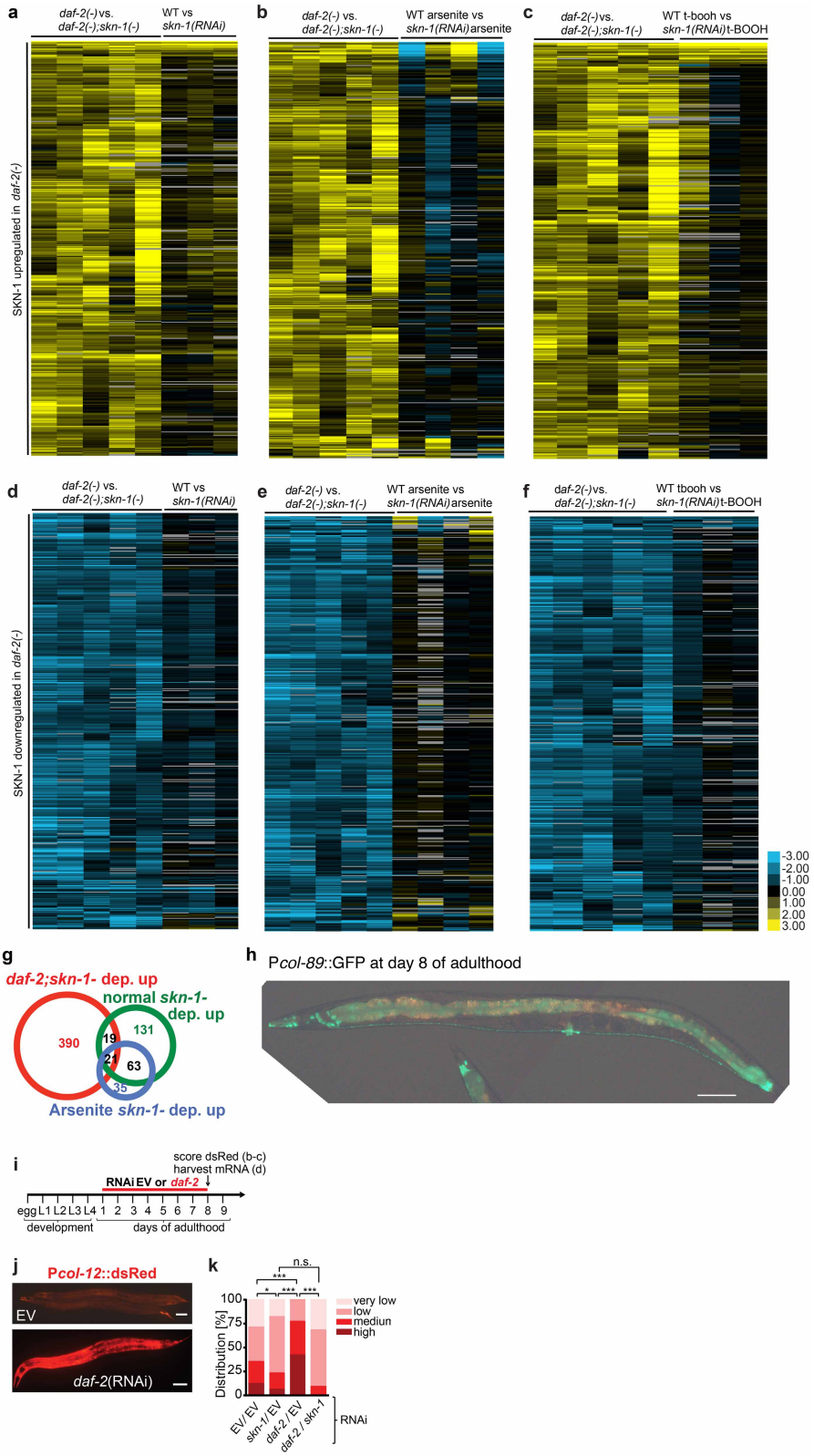

Extended Data Figure 3 | Analyses of SKN-1-regulated *daf-2*(−) genes. **a**–**f**, SKN-1-upregulated (**a**–**c**) and downregulated (**d**–**f**) *daf-2*(−) gene sets were examined by hierarchical clustering to determine how they were previously found to be affected by SKN-1 under unstressed or oxidative stress conditions[18]. t-BOOH, *tert*-butyl hydroperoxide. **g**, Proportional Venn diagrams show comparisons of SKN-1-upregulated genes identified under *daf-2*(−), normal, or arsenite treatment conditions[18] (Supplementary Table 7). In each case, L4 larvae were analysed to avoid embryogenesis effects. Heatmaps are shown in **a**–**f**. **h**, The SKN-1-upregulated *daf-2*(−) collagen *col-89* is expressed in neurons and the intestine, but not in hypodermis. Transgenic P*col-89*::GFP (BC12533) at day 8 of adulthood is shown. Anterior to the left, ventral side down; scale bar, 100 μm. **i**–**k**, SKN-1-mediated collagen gene activation in day 8 *daf-2*(*RNAi*) adults. Adulthood *daf-2* knockdown (**i**) activated a P*col-12*::dsRED reporter (**j**; scale bar, 100 μm). **k**, The *skn-1* dependence of P*col-12*::dsRED expression. EV, empty RNAi vector. $N > 60$ for each condition, three merged trials, with P value by χ^2 test (*$P < 0.05$; ***$P < 0.0001$; n.s., not significant).

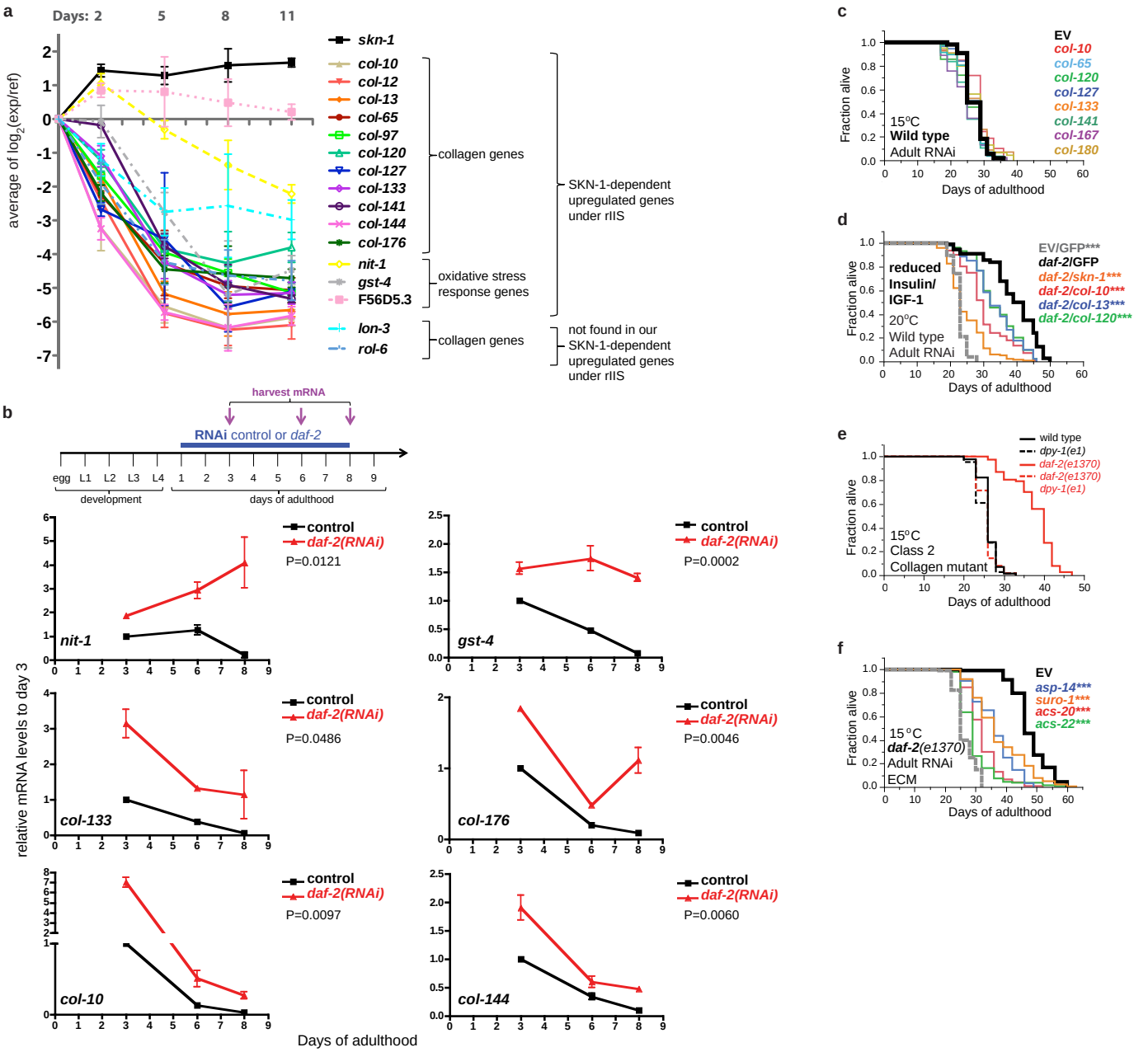

Extended Data Figure 4 | rIIS delays age-associated decline in collagen expression. **a**, Age-associated decline in expression of selected collagen and SKN-1-dependent detoxification genes. Eighty-eight collagens are among many genes that decline in expression as *C. elegans* ages[22]. Fifty of these age-downregulated genes were in our SKN-1 upregulated *daf-2*(−) gene set, including 27 collagen genes (Supplementary Table 10). These *daf-2*(−); SKN-1-dependent collagens were neither flanked by SKN-1 binding sites nor bound by SKN-1 in a genome-wide survey (Supplementary Table 9)[70], suggesting that they are regulated by SKN-1 indirectly. The average Cy5-labelled cDNA values of day 2–11 adults (indicated as 'exp') are plotted in binary logarithm ($\log_2$) relative to cy3-labelled reference cDNA from mixed stage hermaphrodites (indicated as 'ref'). Data are from ref. 22. The *nit-1*, *gst-4*, and *F56D5.3* genes are predicted to encode a nitrilase, glutathione *S*-transferase, and NADPH oxidoreductase, respectively (WormBase). **b**, Expression of SKN-1-regulated collagen and oxidative stress response genes (*nit-1* and *gst-4*) are maintained during ageing in *daf-2*(*RNAi*) animals. One-day-old adult wild-type (N2) animals were placed on either empty vector control (L4440) (black) or *daf-2* RNAi (red) at 20 °C. mRNA was harvested at days 3, 6, and 8. mRNA levels are shown relative to wild-type (N2) day 3 adults on empty vector control (L4440) RNAi and are represented as mean ± s.e.m. For each condition, two biological samples of more than 100 worms each were analysed by qPCR. For each gene, the statistical difference of relative mRNA expression levels between L4440 and *daf-2*(*RNAi*) treatment over the time course (days 3, 6, 8) is shown by two-way ANOVA (repeated measures). **c**, Adulthood knockdown of SKN-1-upregulated collagens did not affect wild-type lifespan For statistics and additional trials, see Extended Data Table 3 and Supplementary Table 13. **d**, Importance of SKN-1-upregulated collagens for *daf-2*(*RNAi*) longevity. Adulthood RNAi knockdown of *daf-2* combined with collagens or *skn-1* at 20 °C is shown. GFP was the RNAi control. For statistics and additional data, see Supplementary Table 13. **e**, Suppression of *daf-2*(*e1370*) but not wild-type longevity at 15 °C by the collagen mutation *dpy-1*(*e1*), which affects the cuticle[31,75], but was not present in our SKN-1-regulated gene set. For details and statistics see Supplementary Table 13. **f**, Longevity of *daf-2*(*e1370*) at 15 °C requires the SKN-1-upregulated extracellular proteases *asp-14* and *suro-1*, along with cuticle integrity genes *acs-20* and *acs-22* (ref. 62), suggesting a general importance of ECM gene expression. For details and statistics see Supplementary Table 13.

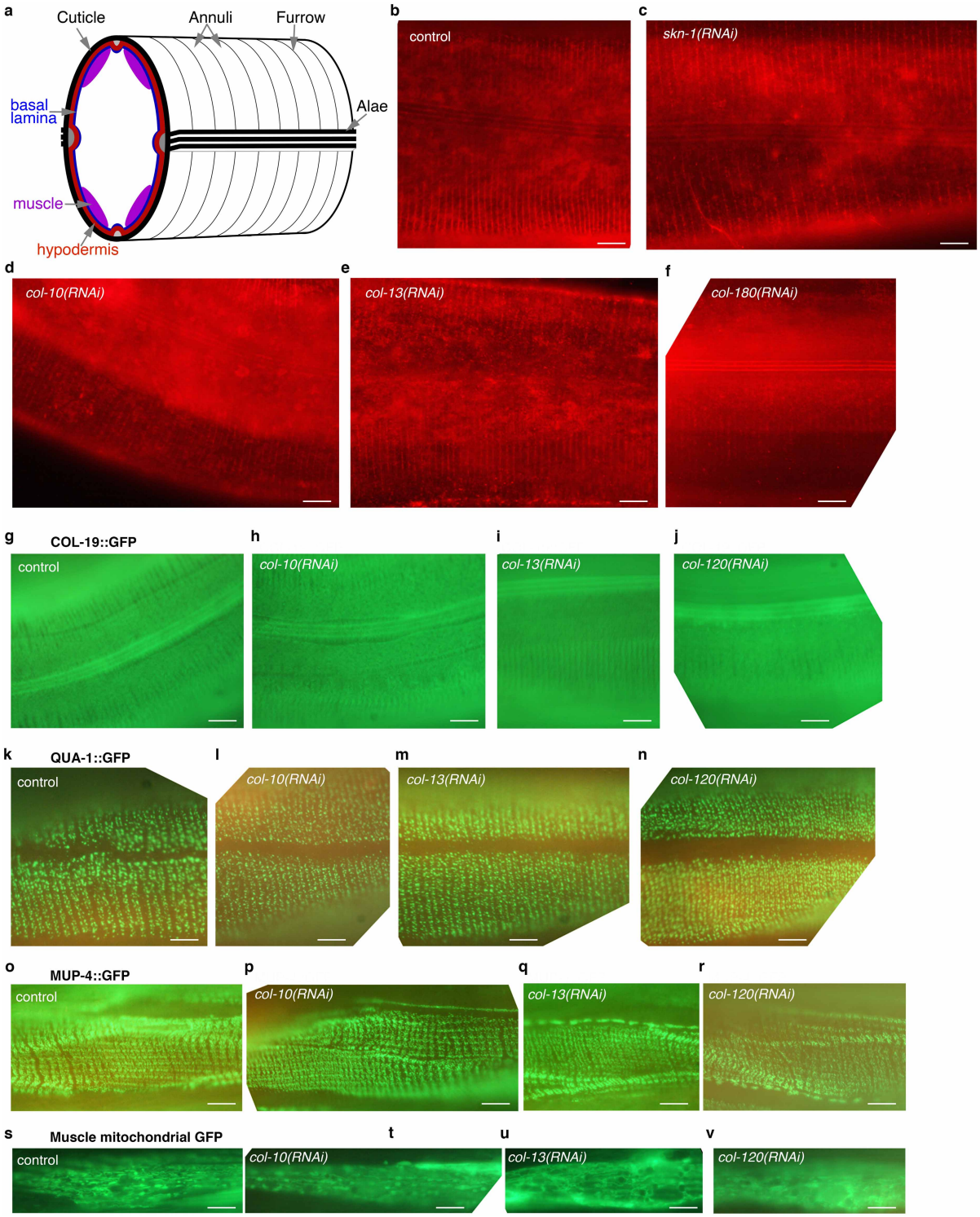

Extended Data Figure 5 | Adulthood knockdown of collagens important for longevity does not affect morphology of cuticle-associated structures. **a**, Schematic cross-section of *C. elegans* illustrating the proximity of the cuticle (black), hypodermis (red), basal lamina (blue), and body-wall muscles (purple). Annuli, furrow, and alae are characteristic cuticle structures. **b**–**j**, Adulthood RNAi against SKN-1-upregulated *daf-2*(−) collagens does not affect cuticle morphology. **b**–**f**, One-day-old wild-type animals were exposed to either empty vector (control) or the indicated RNAi clone by feeding. Ten days later, animals were incubated in DiI for 16 h; the cuticle was imaged as described in ref. 76. $N > 30$ animals per condition scored, with typical images shown. Scale bar, 10 μm. **g**–**j**, Cuticle morphology revealed by the collagen COL-19, detected by a translational fusion protein (*kaIs12* [COL-19::GFP]). We did not identify *col-19* as being regulated by *daf-2* and *skn-1*, and *daf-2*(*RNAi*) did not detectably alter COL-19::GFP levels (not shown). **k**–**n**, Adulthood knockdown of SKN-1-upregulated *daf-2*(−) collagens does not affect the pattern of *chEx1682* QUA-1::GFP, a marker of cuticle adhesion. QUA-1 encodes a hedgehog-related protein required for moulting, cuticle adhesion, and alae formation[42]. **o**–**r**, Adulthood RNAi against SKN-1-upregulated *daf-2*(−) collagens does not affect the pattern of muscle–hypodermis–cuticle adhesion, as indicated by *upIs1* MUP-4::GFP. MUP-4 is a transmembrane protein that is part of a complex that attaches hypodermis and muscles to the cuticle[35]. **s**–**v**, Adulthood collagen knockdown does not affect mitochondrial morphology in muscle. For **g**–**v**, animals were placed on RNAi at the first day of adulthood and scored and imaged at day 8 of adulthood. $N > 30$ animals per condition scored, with typical images shown. Scale bar, 10 μm.

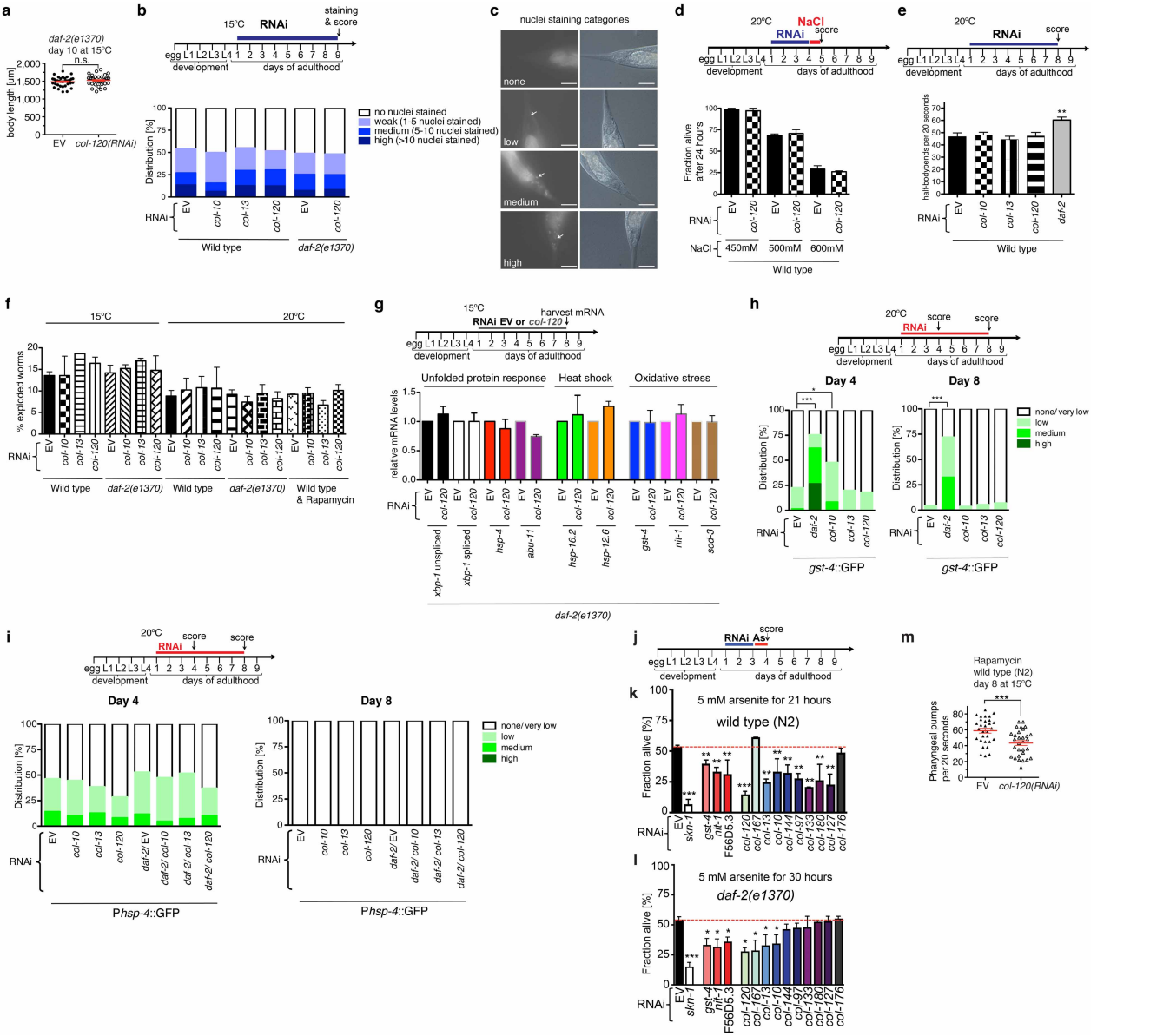

Extended Data Figure 6 | Phenotypic analyses of collagens important for longevity. **a**, Adulthood *col-120* knockdown does not affect *daf-2*(*e1370*) body size at 15 °C. The *daf-2*(*e1370*) animals were placed on RNAi food as day 1 adults, and at day 10 body size, pharyngeal pumping, and lipofuscin levels were scored in parallel in the same animals ($N > 30$; one trial; see Fig. 4a, b). **b**, **c**, Adulthood knockdown of SKN-1-upregulated collagens does not alter barrier function. **b**, Upper panel: animals were placed on RNAi food on adulthood day 1, and at day 9 were incubated in 1 μg ml^{-1} Hoechst 33342, which is membrane-permeable but cuticle-impermeable. For details see Methods, adapted from ref. 62. Lower panel: barrier permeability was not affected by *daf-2* mutation or collagen knockdown. Permeability was assessed by nuclear Hoechst staining in the tail[62] ($N > 50$ per condition; one trial). Approximately half of the animals in each group showed nuclear staining in the tail that is likely to have arisen through uptake in the intestine, as suggested by the high levels of intestinal Hoechst staining (**c**). Uptake through the cuticle would have resulted in a much wider distribution of stained nuclei. **c**, Representative pictures of quantification categories. Arrow indicates Hoechst-stained tail nuclei. Scale bar, 50 μm. **d**, Adulthood knockdown of *col-120* did not sensitize to hypertonic stress. Day 1 adult wild-type animals were placed RNAi food for 3 days, then on plates containing food and high concentrations of salt for 24 h before assay (NaCl: 450 mM, 500 mM, 600 mM; $N > 60$ per condition; two trials). **e**, Adulthood knockdown of SKN-1-upregulated collagens did not impair body movement. Neither the frequency nor morphology (not shown) of body movement was affected. In parallel, the *daf-2* RNAi control increased movement frequency because these animals were chronologically younger. (**$P < 0.001$, one-way ANOVA post hoc Tukey's test compared with empty RNAi vector.) **f**, Adulthood collagen RNAi did not increase vulval rupturing during ageing. The bar graph shows the mean ± s.e.m. percentage of exploded worms that were censored during lifespan assays (Extended Data Table 3 and Supplementary Table 13). **g**–**i**, Adulthood *col-120* knockdown did not induce unfolded protein, heat-shock stress, or oxidative stress responses. In **g**, *daf-2*(*e1370*) mutants were placed on RNAi food as day 1 adults, and assayed at day 8 (upper panel). Relative levels of these stress response gene mRNAs were determined by qPCR (two independent trials, each with 200 worms per condition). **h**, Adulthood collagen RNAi does not activate the oxidative stress response marker P*gst-4*::GFP[34], assayed after 4 and 8 days of RNAi. As a control, *daf-2* RNAi induced SKN-1 to increase *gst-4* expression (Fig. 2a). **i**, Adulthood collagen RNAi does not activate the unfolded protein response marker P*hsp-4*::GFP[40]. **j**–**l**, Importance of collagens for oxidative stress resistance. Day 1 adults were exposed to empty vector (EV) or RNAi food at 15 °C, then at day 3 were placed in 5 mM arsenite (As) and scored for survival. Knockdown of collagens and other SKN-1 upregulated *daf-2*(−) genes sensitized to oxidative stress from arsenite; *nit-1* (nitrilase), *gst-4* (glutathione *S*-transferase), *F56D5.3* (NADPH oxidoreductase). *$P < 0.05$, **$P < 0.01$, ***$P < 0.001$ relative to control (empty RNAi vector), determined by one-way ANOVA with post hoc Tukey's test. t-BOOH experiments are described in Supplementary Table 16. **m**, Adulthood collagen expression required for rapamycin to delay appearance of an ageing marker (pharyngeal pumping). $N > 30$; each dot represents an animal; ***$P < 0.0001$ determined with an unpaired *t*-test, two-tailed.

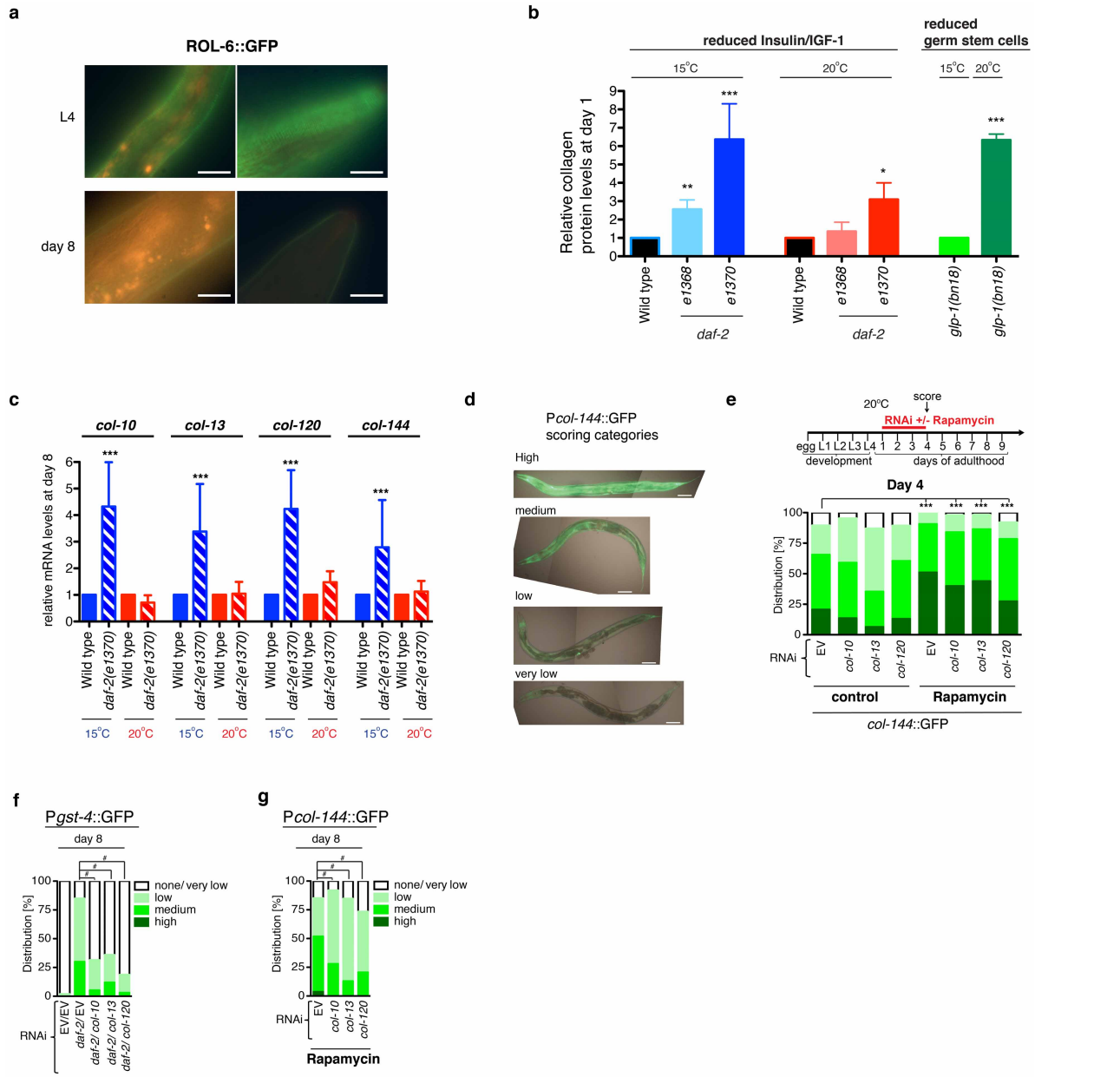

Extended Data Figure 7 | Cuticle remodelling in adults a, The collagen ROL-6 is present in the cuticle during development and early adulthood[77], then largely disappears during ageing. The upper panels show the mid-body (left) and head (right) regions in an L4 animal. Day 1 adults exhibited similar levels and patterns of *jgIs5* ROL-6::GFP fluorescence (not shown). Lower panels show the corresponding regions in a day 8 adult, in which *jgIs5* ROL-6::GFP levels are reduced. The orange signal corresponds to gut autofluorescence. Representative images are shown; scale bar, 20 µm. $N = 30$ for each sample set (L4, day 1, and day 8). **b**, Total collagen levels are elevated in long-lived animals at the first day of adulthood. Note that these long-lived animals also maintain higher collagen levels in later life despite an age-related decline (Fig. 4d). Relative collagen levels were estimated by a hydroxyproline assay[61]. In *daf-2* mutants, total collagen levels were elevated at both temperatures but the increase was greater at 15 °C, at which *skn-1* and SKN-1-dependent collagens are required for lifespan extension (Fig. 3 and Supplementary Table 13). Temperature-sensitive *glp-1*(*bn18*) mutants were maintained at 15 °C (permissive temperature), or upshifted to 25 °C (restrictive temperature) as L1 larvae until the L4 stage, then placed at 20 °C. **c**, SKN-1-dependent collagen genes from the *daf-2*(−) set are not upregulated in 8-day-old *daf-2*(*e1370*) adults at 20 °C. Expression of these collagens remains increased at this age in *daf-2*(*e1370*) at 15 °C or after *daf-2* RNAi at 20 °C (Fig. 2a and Extended Data Figs 2c and 4b), conditions in which the dauer pathway is inactive and lifespan extension is *skn-1* dependent (see text). Two hundred day-8 adults were assayed in each sample, with three merged independent trials shown. **d**, Scoring categories for the P*col-144*::GFP reporter are shown in (**e**, **g**; Fig. 4f; scale bar, 100 µm). **e**, Adulthood rapamycin treatment increases *col-144* promoter activity. Knockdown of *col-10*, *col-13*, or *col-120* did not reduce P*col-144*::GFP levels at day 4, but significantly decreased P*col-144*::GFP levels by day 8 (**g**). $N > 60$ for each condition, two merged trials, with P value by χ^2 test ($^{\#}P < 0.0001$ against untreated empty RNAi vector control animals). **f**, Dependence of the SKN-1 target gene *gst-4* on adulthood SKN-1-upregulated collagen expression in *daf-2*(*RNAi*) animals. Collagen or empty vector (EV) control RNAi was initiated at day 1 of adulthood at 20 °C, together with *daf-2* knockdown. **g**, Adulthood collagen RNAi decreases *col-144* promoter activity in rapamycin-treated animals. As is seen in *daf-2* mutants at 15 °C (Fig. 4f), activity of this rapamycin-activated promoter is unaffected by adulthood collagen RNAi at day 4 (**e**), but reduced at day 8. For **f** and **g**, $N > 60$ for each condition, two merged trials, with P value by χ^2 test ($^{\#}P < 0.0001$).

Extended Data Table 1 | The *skn-1* dependence of *daf-2* lifespan extension in the absence of dauer-related mechanisms

Strain	Temp [°C]	Mean lifespan ± S.E.M. [Days]	75th per-centile [Days]	N assayed / Initial N	% mean lifespan change to N2 or control	% mean lifespan change to *skn-1*	P-value (log-rank) vs. N2	P-value (log-rank) vs. *skn-1*	P-value (log-rank) vs. *daf-2*	Figure
3 merged trials at 15°C *										
wild type (N2)	15	23.4 ± 0.3	27	279/332						1a
skn-1(zu67)	15	16.9 ± 0.2	19	278/315	-28		<0.0001			1a
daf-2(e1370)	15	36.7 ± 0.5	44	372/396	+57	+117	<0.0001	<0.0001		1a
daf-2(e1370); skn-1(zu67)	15	17.1 ±0.2	19	308/327		+1	<0.0001	0.7993	<0.0001	1a
Trial at 15°C and 20°C										
wild type (N2) L4440(RNAi)	15	25.4 ± 0.5	27	74/83						
wild type (N2) *daf-2*(RNAi)	15	39.1 ± 1.2	42	64/73	+54	+146	<0.0001	<0.0001		
skn-1(tm3411) L4440(RNAi)	15	15.9 ± 0.4	16	116/136	-37		<0.0001		<0.0001	
skn-1(tm3411) daf-2(RNAi)	15	16.6 ± 0.7	16	84/103		+6	<0.0001	0.6424	<0.0001	
wild type (N2) L4440(RNAi)	**20**	23.6 ± 0.5	26	45/51						1b
wild type (N2) *daf-2*(RNAi)	**20**	34.8 ± 1.1	40	45/50	+47	+120	<0.0001	<0.0001		1b
skn-1(tm3411) L4440(RNAi)	**20**	15.8 ± 0.5	16	93/108	-33		<0.0001		<0.0001	1b
skn-1(tm3411) daf-2(RNAi)	**20**	17.1 ± 0.5	16	115/124		+8	<0.0001	0.0491	<0.0001	1b
Trial at 20°C										
wild type (N2) L4440(RNAi)	**20**	23.3 ± 0.2	23	67/74						
wild type (N2) *skn-1*(RNAi)	**20**	18.6 ± 0.2	19	96/101	-20		<0.0001			ED 1f
daf-16(mu86);daf-2(e1370) L4440(RNAi)	**20**	17.0 ± 0.2	19	73/83	-27	-9	<0.0001	<0.0001	<0.0001	ED 1f
daf-16(mu86);daf-2(e1370) skn-1(RNAi)	**20**	16.5 ± 0.2	19	78/89	-29	-11	<0.0001	<0.0001	<0.0001	
daf-2(e1370) L4440(RNAi)	**20**	41.7 ± 0.9	47	82/87	+79	+124	<0.0001	<0.0001		ED 1f
daf-2(e1370) skn-1(RNAi)	**20**	38.9 ± 0.8	42	96/102	+67	+109	<0.0001	<0.0001	0.0153	ED 1f
DAF-16 rescued in all tissues: *daf-16(mgDf50);daf-2(e1370); Ipls14* [P*daf-16*::DAF-16f::GFP] L4440(RNAi)	**20**	53.5 ± 1.0	61	77/83	+130	+188	<0.0001	<0.0001	<0.0001	
DAF-16 rescued in all tissues: *daf-16(mgDf50);daf-2(e1370); Ipls14* [P*daf-16*::DAF-16f::GFP] *skn-1*(RNAi)	**20**	50.8 ± 0.9	58	86/93	+118	+173	<0.0001	<0.0001	<0.0001	
DAF-16 rescued in neurons: *daf-16(mu86);daf-2(e1370); muEx169* [P*unc119*::GFP::DAF-16] L4440(RNAi)	**20**	16.4 ± 0.2	17	71/77	-30	-12	<0.0001	<0.0001	<0.0001	
DAF-16 rescued in neurons: *daf-16(mu86);daf-2(e1370); muEx169* [P*unc119*::GFP::DAF-16] *skn-1*(RNAi)	**20**	16.5 ± 0.2	17	92/97	-29	-11	<0.0001	<0.0001	<0.0001	
DAF-16 rescued in intestine: *daf-16(mu86);daf-2(e1370); muEx211* [P*ges-1*::GFP::DAF-16] L4440(RNAi)	**20**	27.5 ± 0.6	30	89/98	+18	+48	<0.0001	<0.0001	<0.0001	ED 1f
DAF-16 rescued in intestine: *daf-16(mu86);daf-2(e1370); muEx211* [P*ges-1*::GFP::DAF-16] *skn-1*(RNAi)	**20**	18.5 ± 0.3	19	86/93	-21	-0.5	<0.0001	0.2671	<0.0001	ED 1f
Trial at 15°C and 20°C										
wild type (N2) L4440(RNAi)	**15**	24.5 ± 0.6	28	68/76						1c
wild type (N2) *daf-2*(RNAi)	**15**	47.8 ± 1.3	57	81/94	+95	+148	<0.0001	<0.0001	<0.0001$	1c
skn-1(zu135) L4440(RNAi)	**15**	19.3 ± 0.9	21	61/73	-21		<0.0001		<0.0001$	1d
skn-1(zu135) daf-2(RNAi)	**15**	20.3 ± 1.1	26	68/77	-17	+5	0.0026	0.3805	<0.0001$	1d
daf-2(e1368) L4440(RNAi)	**15**	32.9 ± 0.9	40	65/72	+34	+70	<0.0001	<0.0001		1c
daf-2(e1368) daf-2(RNAi)	**15**	71.7 ± 2.3	82	70/78	+193	+272	<0.0001	<0.0001	<0.0001$	1c
daf-2(e1368); skn-1(zu135) L4440(RNAi)	**15**	19.9 ± 0.7	26	48/57	-19	+3	0.0002	0.4624	<0.0001$	1d
daf-2(e1368); skn-1(zu135) daf-2(RNAi)	**15**	19.3 ± 0.9	26	60/65	-21	0	0.0004	0.7268	<0.0001$	1d
wild type (N2) L4440(RNAi)	**20**	22.9 ± 0.3	24	64/75						
wild type (N2) *daf-2*(RNAi)	**20**	38.9 ± 0.7	45	82/91	+69	+133	<0.0001	<0.0001	<0.0001$	
skn-1(zu135) L4440(RNAi)	**20**	16.7 ± 0.2	17	93/104	-27		<0.0001		<0.0001$	
skn-1(zu135) daf-2(RNAi)	**20**	16.6 ± 0.2	17	101/112	-28	-0.6	<0.0001	0.6062	<0.0001$	
daf-2(e1368) L4440(RNAi)	**20**	33.4 ± 0.9	38	51/63	+46	+100	<0.0001	<0.0001		
daf-2(e1368) daf-2(RNAi)	**20**	54.8 ± 0.9	64	62/73	+139	+228	<0.0001	<0.0001	<0.0001$	
daf-2(e1368); skn-1(zu135) L4440(RNAi)	**20**	21.6 ± 0.6	26	112/124	-6	+29	0.7408	<0.0001	<0.0001$	
daf-2(e1368); skn-1(zu135) daf-2(RNAi)	**20**	25.9 ± 1.2	36	81/94	+13	+55	0.0678	<0.0001	<0.0001$	
Trial of crude dauer pheromone at 25°C										
wild type (N2) L4440(RNAi) control	**25**	12.9 ± 0.4	14	30/30						
wild type (N2) L4440(RNAi) crude dauer pheromone	**25**	17.7 ± 0.8	21	30/30	+37	+50	<0.0001	<0.0001		
wild type (N2) *daf-2*(RNAi) control	**25**	21.1 ± 0.7	24	30/30	+64	+79	<0.0001	<0.0001		
wild type (N2) *daf-2*(RNAi) crude dauer pheromone	**25**	25.6 ± 0.9	28	29/30	+98	+117	<0.0001	<0.0001	<0.0001	
skn-1(zu135) L4440(RNAi) control	**25**	11.8 ± 0.3	13	29/30	-9		0.0235		<0.0001	1e
skn-1(zu135) L4440(RNAi) crude dauer pheromone	**25**	16.2 ± 0.6	19	29/30	+26	+37	<0.0001	<0.0001	<0.0001	1e
skn-1(zu135) daf-2(RNAi) control	**25**	12.2 ± 0.4	13	29/30	-5	+3	0.2311	0.4030	<0.0001	1e
skn-1(zu135) daf-2(RNAi) crude dauer pheromone	**25**	16.1 ± 0.6	21	29/30	+25	+36	<0.0001	<0.0001	<0.0001	1e

Lifespans were measured from the L4 stage, and animals that left the plates, buried into the agar, bagged, or exploded were censored. Analyses performed in parallel are grouped. L4440 empty vector was used as the RNAi control. Each *skn-1* mutant analysed is a strong loss-of-function and possible null. The class 2 alleles *daf-2*(*e1370*) and *daf-2*(*m596*) have comparably extended lifespans at 20 °C and 15 °C (Supplementary Table 2). The *daf-2(e1370);skn-1* double mutants lived 55% longer at 20 °C than at 15 °C (Supplementary Table 2), because *skn-1*-independent dauer-related processes increase their lifespan at the higher temperature (see text). This finding is striking given that *C. elegans* generally lives longer at lower temperatures[1] (Supplementary Table 2). Previous analyses of these transgenically rescued *daf-16* strains showed that DAF-16 expression specifically in neurons rescues the dauer but not longevity phenotypes of *daf-2*(*e1370*), whereas intestine-specific DAF-16 rescue allows lifespan extension but not dauer entry[15]. *N*, number of animals observed. *A merger of three trials shown in Supplementary Table 2. ED indicates data shown in an Extended Data Figure. *P* values were determined by log-rank. Additional experiments are shown in Supplementary Table 2.

Extended Data Table 2 | Collagen genes are upregulated by diverse interventions that increase lifespan

Experimental condition	Total # of genes upregulated	Reference	Enrichment score rank of collagens	# of collagens upregulated	# of collagens shared with *daf-2; skn-1* upregulated collagens	shared collagens tested in lifespan assays (in this study)
COLLAGENS UPREGULATED BY DRUG TREATMENTS THAT INCREASE *C. ELEGANS* LIFESPAN						
Resveratrol treatment in young wild-type adults	116	[78]	2	**8**	0	
Resveratrol treatment in young *daf-16(-)* adults	1027	[78]	1	**85**	28	*col-12, col-13, col-65, col-97, col-120, col-127, col-133,*
Humic acid treatment in 11 days old wild-type adults	740	[79]	1	**27**	5	*col-13, col-167, col-133*
Tannic acid treatment in young wild-type adults	2842	[80]	1	**74**	33	*col-10, col-12, col-13, col-65, col-97, col-133, col-141, col-144, col-167, col-180*
Quercetin treatment in young wild-type adults	1562	[80]	1	**67**	18	*col-12, col-13, col-97, col-133*
MAHMA (nitric oxide donor) in wild-type L4 worms	65	[81]	1	**8**	1	*col-97*
MAHMA (nitric oxide donor) in *hsf-1(sy441)* L4 worms	99	[81]	1	**21**	1	*col-97*
Rotenone treatment in young wild-type adults	2380	[82]	1	**64**	27	*col-10, col-65, col-97, col-133, col-141*
COLLAGENS UPREGULATED IN GENETIC BACKGROUNDS THAT INCREASE *C. ELEGANS* LIFESPAN						
Mixed-stage ***wdr-23****(tm1817)* mutants compared to wild type	2285	[83]	7	**41**	15	*col-10, col-144, col-167*
Young ***age-1****(mg44)* adults compared to wild type	791	[84]	1	**54**	9	*col-141*
daf-2(e1370) at day 5 of adulthood vs wild type*	869	[85]	1	**57**	19	*col-10, col-12, col-65, col-89, col-97, col-144, col-167*
daf-2*(m41)* at day 10 vs. wild type at day 6 of adulthood at 25.5°C	48	[86]	2	**17**	1	*col-141*
DAF-16-dependent genes expressed in ***daf-2(e1370)*** in day 1 adults at 20°C**	1078	[74]	1	**43**	16	*col-141*
TGFβ-dependent in day 1 adults	2181	[74]	1	**90**	30	*col-13, col-65, col-127, col-141, col-144, col-167, col-180*
AMPK and downstream signaling (shared transcriptional output of loss of *crh-1* (CREB) / loss of *tax-6* (calrectulin) / AAK-2 (AMPK) overexpression) in L4 larvae	549	[87]	1	**31**	17	*col-12, col-13, col-127, col-133, col-141, col-167, col-180*
ash-2 RNAi in animals that lacked a germline in day 8 adults	592	[88]	1	**21**	4	*col-12, col-133*
Young ***isp-1*** mutant adults compared to wild type	709	[89]	3	**15**	2	
cyc-1 RNAi in young adults	2459	[89]	1	**51**	18	*col-12, col-13, col-97, col-120, col-141, col-144*
2 day old ***rsks-1****(ok1255)* adults	155	[90]	1	**13**	3	*col-133*
Young ***ctbp-1****(ok498)* adults	213	[91]	1	**30**	16	*col-65, col-97, col-120, col-144, col-180*

Collagens were overrepresented in each *C. elegans* longevity-associated gene set we examined[74,78–91]. Gene Ontology (GO) enrichment clusters were identified by DAVID, using high-stringency classification. Enrichment scores were ranked from highest (1) to lowest (>10). Additional information is provided in Supplementary Table 10, including *P* values that were determined by DAVID using Fisher's exact test[53,92,93]. *Temperature not specified. **A comparison of *daf-2*(*e1370*) versus *daf-16*(*mu86*)*; daf-2*(*e1370*).

Extended Data Table 3 | Suppression of lifespan extension by adulthood collagen gene knockdown

Strain / **RNAi**	Mean lifespan ± S.E.M. [Days]	75th percentile [Days]	N dead/ Initial N	% mean lifespan change to control	P-value (log-rank) vs. control	Figure
Trial of collagen genes from SKN-1-upregulated *daf-2(-)* set at 15°C						
rrf-3(pk1426) RNAi **L4440 (control)**	27.2 ± 0.4	29	55/64			ED Fig. 4c
rrf-3(pk1426) RNAi ***col-10***	28.2 ± 0.6	29	70/77	+4	0.0253	ED Fig. 4c
rrf-3(pk1426) RNAi ***col-65***	26.4 ± 0.5	29	57/70	-3	0.4555	ED Fig. 4c
rrf-3(pk1426) RNAi ***col-120***	25.7 ± 0.7	29	46/56	-6	0.2542	ED Fig. 4c
rrf-3(pk1426) RNAi ***col-127***	26.7 ± 0.5	29	48/61	-2	0.4797	ED Fig. 4c
rrf-3(pk1426) RNAi ***col-133***	27.2 ± 0.7	31	58/69	0	0.4623	ED Fig. 4c
rrf-3(pk1426) RNAi ***col-141***	25.3 ± 0.8	29	29/43	-7	0.0668	ED Fig. 4c
rrf-3(pk1426) RNAi ***col-167***	24.8 ± 0.7	29	47/64	-9	0.1128	ED Fig. 4c
rrf-3(pk1426) RNAi ***col-180***	27.3 ± 0.7	29	47/61	0	0.4668	ED Fig. 4c
			P-value and % mean lifespan change are relative to *rrf-3(pk1426)* RNAi L4440			
daf-2(e1370); rrf-3(pk1426) RNAi **L4440**	37.3 ± 1.1	43	51/62			Fig. 3a
daf-2(e1370); rrf-3(pk1426) RNAi ***col-10***	28.6 ± 0.6	31	69/80	-23	<0.0001	Fig. 3a
daf-2(e1370); rrf-3(pk1426) RNAi ***col-65***	30.4 ± 0.8	36	71/86	-18	<0.0001	Fig. 3a
daf-2(e1370); rrf-3(pk1426) RNAi ***col-120***	26.6 ± 0.6	29	53/66	-29	<0.0001	Fig. 3a
daf-2(e1370); rrf-3(pk1426) RNAi ***col-127***	29.5 ± 0.7	33	56/62	-21	<0.0001	Fig. 3a
daf-2(e1370); rrf-3(pk1426) RNAi ***col-133***	28.2 ± 0.5	31	66/75	-24	<0.0001	Fig. 3a
daf-2(e1370); rrf-3(pk1426) RNAi ***col-141***	29.1 ± 0.6	31	58/71	-22	<0.0001	Fig. 3a
daf-2(e1370); rrf-3(pk1426) RNAi ***col-167***	28.3 ± 0.6	29	50/59	-24	<0.0001	Fig. 3a
daf-2(e1370); rrf-3(pk1426) RNAi ***col-180***	30.7 ± 0.7	33	53/65	-18	<0.0001	Fig. 3a
			P-value and % mean lifespan change are relative to *daf-2(e1370); rrf-3(pk1426)* RNAi L4440			
eat-2(ad1116); rrf-3(pk1426) RNAi **L4440**	42.1 ± 1.0	47	75/81			Fig. 3c
eat-2(ad1116); rrf-3(pk1426) RNAi ***col-10***	38.9 ± 0.9	45	97/102	-7	0.0356	Fig. 3c
eat-2(ad1116); rrf-3(pk1426) RNAi ***col-65***	38.0 ± 1.0	43	75/79	-10	0.0038	Fig. 3c
eat-2(ad1116); rrf-3(pk1426) RNAi ***col-120***	37.1 ± 0.9	43	60/64	-12	<0.0001	Fig. 3c
eat-2(ad1116); rrf-3(pk1426) RNAi ***col-127***	37.4 ± 0.8	43	83/85	-11	<0.0001	Fig. 3c
eat-2(ad1116); rrf-3(pk1426) RNAi ***col-133***	37.3 ± 1.1	45	75/83	-11	0.0022	Fig. 3c
eat-2(ad1116); rrf-3(pk1426) RNAi ***col-141***	34.7 ± 1.2	43	49/54	-18	<0.0001	Fig. 3c
eat-2(ad1116); rrf-3(pk1426) RNAi ***col-167***	36.9 ± 1.0	43	62/69	-12	0.0002	Fig. 3c
eat-2(ad1116); rrf-3(pk1426) RNAi ***col-180***	34.5 ± 0.9	37	55/58	-18	<0.0001	Fig. 3c
			P-value and % mean lifespan change are relative to *eat-2(ad1116); rrf-3(pk1426)* RNAi L4440			
Trial of collagen genes from SKN-1-upregulated *daf-2(-)* set at 20°C						
wild type (N2) RNAi **L4440 (control)**	24.6 ± 0.2	25	98/107			Fig. 3b
daf-2(e1370); rrf-3(pk1426) RNAi **L4440**	38.2 ± 0.8	44	86/93			Fig. 3b
daf-2(e1370); rrf-3(pk1426) RNAi ***col-10***	37.4 ± 0.7	42	104/110	-2	0.4014	Fig. 3b
daf-2(e1370); rrf-3(pk1426) RNAi ***col-13***	35.2 ± 0.7	42	92/99	-7	0.0043	Fig. 3b
daf-2(e1370); rrf-3(pk1426) RNAi ***col-120***	38.8 ± 0.6	44	103/110	+2	0.9386	Fig. 3b
			P-value and % mean lifespan change are relative to *daf-2(e1370); rrf-3(pk1426)* RNAi L4440			
Trial of collagen genes from the SKN-1-upregulated *daf-2(-)* set at 20°C						
wild type (N2) RNAi **L4440 (control)** 0.2% DMSO	25.7 ± 0.3	29	96/103			Fig. 3d
wild type (N2) RNAi ***col-10*** 0.2% DMSO	25.7 ± 0.4	28	92/100	0	0.1545	
wild type (N2) RNAi ***col-13*** 0.2% DMSO	26.4 ± 0.3	27	102/111	+3	0.0811	
wild type (N2) RNAi ***col-120*** 0.2% DMSO	26.6 ± 0.2	29	98/104	+4	0.0147	
			P-value and % mean lifespan change are relative to wild type (N2) RNAi L4440 (control) 0.2% DMSO			
wild type (N2) RNAi **L4440 (control)** 0.2% DMSO 100μM Rapamycin	30.7 ± 0.3	32	107/118			Fig. 3d
wild type (N2) RNAi ***col-10*** 0.2% DMSO 100μM Rapamycin	28.6 ± 0.5	32	83/93	-7	0.0083	Fig. 3d
wild type (N2) RNAi ***col-13*** 0.2% DMSO 100μM Rapamycin	28.0 ± 0.5	32	83/90	-8	0.0003	Fig. 3d
wild type (N2) RNAi ***col-120*** 0.2% DMSO 100μM Rapamycin	26.8 ± 0.5	29	77/87	-13	<0.0001	Fig. 3d
			P-value and % mean lifespan change are relative to wild type (N2) RNAi L4440 (control) 0.2% DMSO 100μM Rapamycin			
Trial of collagen genes from SKN-1-upregulated *daf-2(-)* set at 20°C						
wild type (N2) RNAi **L4440 (control)**	23.8 ± 0.3	26	126/142			Fig. 3e
wild type (N2) RNAi ***col-10***	23.7 ± 0.3	26	94/108	0	0.9994	
wild type (N2) RNAi ***col-13***	23.3 ± 0.3	26	97/112	-2	0.2122	
wild type (N2) RNAi ***col-120***	23.1 ± 0.3	26	71/84	-3	0.1610	
			P-value and % mean lifespan change are relative to wild type (N2) RNAi L4440 (control)			
glp-1(bn18) RNAi **L4440 (control)**	31.2 ± 0.6	34	53/64			Fig. 3e
glp-1(bn18) RNAi ***col-10***	25.8 ± 0.6	30	74/90	-17	<0.0001	Fig. 3e
glp-1(bn18) RNAi ***col-13***	27.8 ± 0.7	30	64/84	-11	0.0001	Fig. 3e
glp-1(bn18) RNAi ***col-120***	27.0 ± 0.6	30	75/98	-13	<0.0001	Fig. 3e
			P-value and % mean lifespan change are relative to *glp-1(bn18)* RNAi L4440 (control)			

Lifespans were measured and presented as in Extended Data Table 1, and 1-day-old animals were placed on RNAi plates. Additional related experiments are shown in Supplementary Table 13. The *col-10* and *col-12* genes share more than 99% protein sequence identity with *col-144* and *col-13*, respectively. In analysis of *glp-1*(*bn18*), both N2 and *glp-1* animals were upshifted from 15 to 25 °C from the mid-L1 stage until the first day of adulthood, then we analysed lifespan at 20 °C.